PALEOECOLOGICAL RECONSTRUCTION OF THE

BRIDGER RANGE, MONTANA, USA

by

James Victor Benes

A thesis submitted in partial fulfillment
of the requirements for the degree

of

Master of Science

in

Earth Sciences

MONTANA STATE UNIVERSITY

Bozeman, Montana

November 2016

DEDICATION

I dedicate this thesis to my parents. I love you. “Watch me dive!”

ACKNOWLEDGEMENTS

My first acknowledgement of appreciation is for my advisor, Dr. Cathy Whitlock. I appreciate her wellspring of patience as I found my way through the graduate school experience. It has been an incredible journey. I also thank my committee members, who helped guide me along the way, Drs. Greg Pederson, Dave McWethy, and Bill Wyckoff. Next, I'd like to acknowledge Dr. Sheri Fritz, who mentored me during my undergraduate years. Thank you for engendering an interest in paleoclimates, and thank you for guiding me toward graduate school. Along the same lines, I'd like to thank Dr. Tommy Brackins of the U.S. Coast Guard, Ms. Carol Boehler of the University of Nebraska, and Mr. K.C. Bolton. At some time or another, the three of you encouraged me to pursue higher education in order to satiate my curiosities of the world. Thank you for your slight pushes to where I am now.

I would not be writing this thesis if it was not for the lab mates that helped me so tremendously along the way. Dr. Teresa Krause, Dr. Virginia Iglesias, Dr. Gabe Yospin, Ali White, Pico Alt, Buzz Nanavati, Chris Schiller, Bar Ulrich, Dave Firmage, and most importantly, Laurie Stahle.

Field work and lab assistance was provided by Paul Bodalski, Jen Giskaas, James Mauch, Jeff Gay, Matt Weingart, Charles Shama, and Helen K. Dailey. Thank you for your time and energy.

My last acknowledgement goes to my wonderful husband, Tim Turnquist. Without your incredible support, editing, patience, and love, this surely would have been a more difficult endeavor.

TABLE OF CONTENTS

LIST OF TABLES

LIST OF FIGURES

ABSTRACT

The postglacial vegetation and fire history of the Greater Yellowstone Ecosystem (GYE) is poorly known immediately outside of the Yellowstone and Grand Teton national parks due to the scarcity of pollen and charcoal records. The paleoecological record of the Bridger Range near the northwestern GYE boundary provides new information on the ecological history of the region. A 5-m-long sediment core was taken from Fairy Lake (45°54'16.00''N, 110°57'29.00''W, 2306 m elev) to reconstruct the regional vegetation, fire, and climate history. Pollen analysis reveals shifts in vegetation from tundra-steppe to early *Picea* with *Pinus* parkland, and open forest of *Pinus, Pseudotsuga, Abies,* and *Picea* and finally closed forest over the last ca. 15,000 years, similar to other regional pollen records in the GYE. Fluctuations in different conifer species are interpreted as a response to regional climate changes. Wetter, cooler periods are associated with expansion of *Picea*. Warmer periods of time are associated with more open landscapes, and more frequent burning, but with less biomass burnt due to the more open landscape. Changes in the ratio of arboreal pollen to non-arboreal pollen were studied through time from sites spanning a west-to-east transect across the Northern Rocky Mountains (NRM), with Fairy Lake, and other records from the northern GYE in the center. Arboreal pollen is higher in the west, where annual/seasonal rainfall (or available moisture during the growing season) is greater. Charcoal records from the NRM were also compared to Fairy Lake's charcoal record in an effort to distinguish Fairy Lake from other NRM sites. The Fairy Lake fire record is similar to some NRM sites in the late-glacial and late Holocene with increased fire activity along with increases in available biomass. Archeological remains in the Fairy Lake watershed suggest some level of human activity in recent centuries, although the extent of human influence on vegetation change is not easily distinguished from climatic controls.

PALEOECOLOGICAL RECONSTRUCTION OF THE BRIDGER RANGE, MONTANA, USA

Introduction

The Greater Yellowstone Ecosystem (GYE) encompasses about 72,843 km^2 of northwestern Wyoming, southwestern Montana and eastern Idaho. The GYE includes Yellowstone National Park (YNP), Grand Teton National Park (GTNP), the surrounding six national forests and three national wildlife refuges, as well as private, tribal and public lands. The complex topography of the GYE includes the Wind River Range, Wyoming Range, Gallatin Range, Bridger Range, Crazy Mountains, Absaroka Range, and Beartooth Uplift (National Park Service, 2016). Most of our understanding of the vegetation, fire and climate history of this area comes from research within Yellowstone and Grand Teton national parks (Higuera et al., 2010, Huerta et al., 2009, Krause & Whitlock, 2013, Millspaugh et al., 2000, Millspaugh & Whitlock, 1995, Waddington & Wright, 1974, Whitlock et al., 2012, Whitlock et al., 2007, Whitlock, 1993, Whitlock & Bartlein, 1993). By comparison, the vegetation and fire history of the margins surrounding the GYE are not well known, aside from records that lie immediately outside the national parks: Lower Red Rock Lakes in southwestern Montana (Mumma et al., 2012), which was ice-free during the last ice age, and Dailey Lake just north of YNP (Krause et al., 2015), which focused on the late-glacial/early Holocene transition period along with a handful of other records bordering the edge of the parks (Fall et al., 1995, Shuman et al., 2010). This thesis builds on the framework of these and previous studies in the GYE and Northern Rocky Mountains (NRM) by describing a paleoecological record from Fairy Lake in the Bridger Range of southwestern Montana. The objectives are to answer these questions:

1. What is the vegetation and fire history of the Bridger Range?

2. How does the environmental history of the Bridger Range compare with other paleoenvironmental records from the GYE and NRM?

Site Description

The Bridger Range

The Bridger Range forms part of the northeastern border of the Gallatin Valley (Fig. 1) and comprises a 10-km wide ridge with a northwest-southeast alignment that stretches for approximately 40 km (Birkeland & Mock, 1996). The highest peak, Sacagawea Peak, has an elevation of 2948 m. Geologically, the Bridger Range generally contains Precambrian metamorphics, Cambrian, Devonian, Jurassic and Cretaceous limestones, and Mississippian, Pennsylvanian, Jurassic and Cretaceous sandstones, mudstones and shales (McMannis, 1955). In addition, the western side consists of poorly sorted Quaternary fan deposits on Oligocene and Miocene andesite-derived sandstones, siltstones and conglomerates (McMannis, 1955). The eastern side consists of volcanic rocks, sandstones and conglomerates, with outcrops of limestone, all of early Tertiary age. The Bridger Range consists of a series of superimposed folds, thrust faults, and strike-slip faults (McMannis, 1955).

Fairy Lake (45°54'16.00"N, 110°57'29.00"W, 2304 m elev, 4 ha, 12 m water depth) lies in a glacial scour basin on the east side of the Bridger Range, below Sacagawea Peak (K. Pierce, personal communication, 09/2015)(Fig. 1). The lake is fed by surface flow and a small spring-fed stream, and drained by a small outlet stream, Fairy Creek. Watershed geology consists of interbedded shale, siltstone, calcareous sandstones and basal conglomerates of the Jurassic Ellis Group, along with shales and mudstone of the Jurassic Morrison Formation (McMannis, 1955). The Pennsylvanian Big Snowy-Amsden Formation forms cliffs on the southwestern side of the Fairy Lake watershed.

The Bridger Range was partially glaciated during the late Pleistocene (McMannis, 1955). Cirques and glacial moraines provide evidence of alpine glaciation north of Ross Peak in the Bridger Range. Although the exact timing of the last glaciation in the Bridger Range is unknown, it is reasonable to assume that it coincided with the timing of Pinedale Glaciation in the northern Yellowstone National Park region. The late-Pleistocene glacial complex there reached its maximum extent approximately ~17,000 cal yr BP (Licciardi & Pierce, 2008). Glacial moraines from Bull Lake and Pinedale glaciations are identified downslope of Fairy Lake (K. Pierce, personal communication, 09/2015).

Present-day Climate

The northwest alignment of the Madison Range and Beaverhead Mountains to the southwest of the Bridger Range creates orographic barriers for moist Pacific air masses from the west. As a result, a modest rain shadow to the west/southwest of the Bridger

Range exists and reduces the amount of moisture that reaches the west side of the Bridger Range (Birkeland & Mock, 1996).

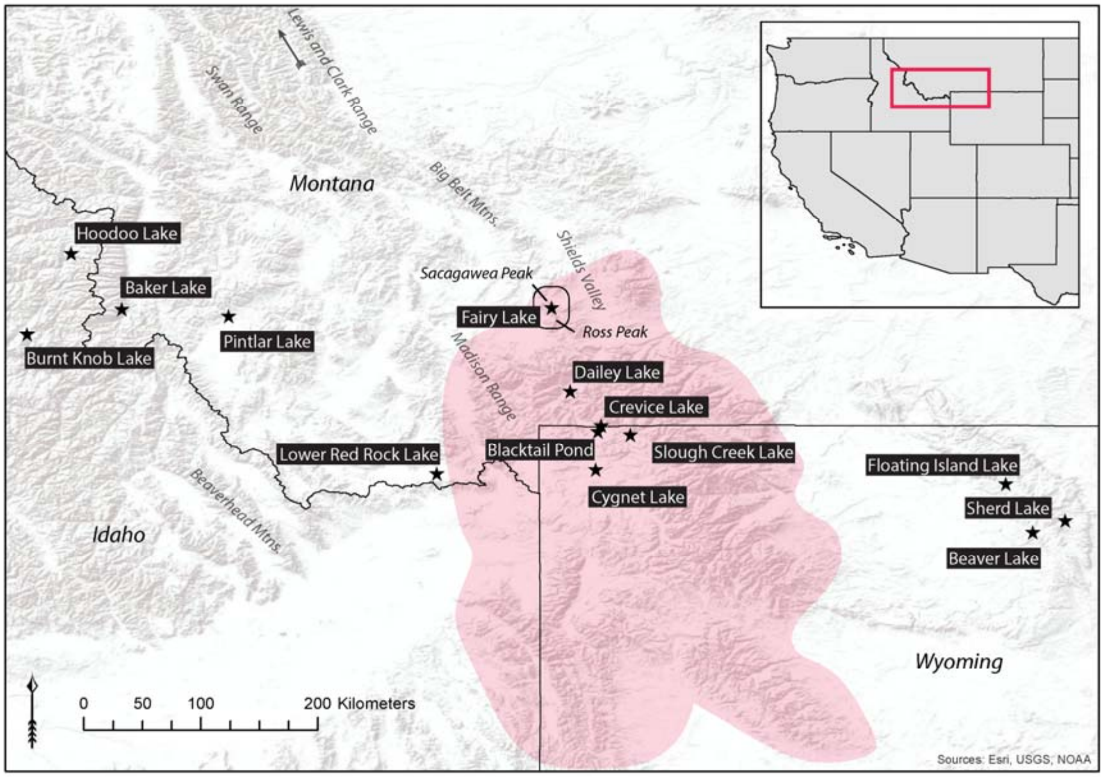

Fig. 1. Fairy Lake and study area. Sites discussed are shown as a black star. Circled area with Fairy Lake in the center demarcates the Bridger Range. Red shading marks the area referred to in this text as the Greater Yellowstone Ecosystem (GYE).

The average maximum summer (June-August) temperature from 1950 to 1995 was 22.3°C, with an average minimum of 3.7°C. Average maximum winter (December-March) temperature was 1.8°C, and the average minimum was -11.5°C (Western Regional Climate Center, 2016). Annual precipitation from 1981-2010 in the Bridger

Range varied from 127-152 cm at elevations of ~2400 – 1800 m and 51-61 cm at elevations of ~1800 – 1500 m (Daly et al., 2008, PRISM Climate Group, 2015).

Two large-scale summertime climatic patterns influence the NRM region, the northeastern Pacific subtropical high-pressure system off the northwestern coast of North America and the monsoonal low-pressure systems in the Gulf of Mexico and Gulf of California (Whitlock & Bartlein, 1993, Mock, 1996, Shinker et al., 2006). In summer, subsidence from the Pacific subtropical high-pressure system creates dry conditions across most of the northwestern U.S., including the southern and central GYE and NRM, while moisture-laden air from the Gulf of Mexico and Gulf of California brings convective storms and precipitation to the eastern and northern portions of the GYE (Whitlock & Bartlein, 1993). These precipitation regimes create different climate conditions at a subregional scale by interacting with local topography. As a result, annual or seasonal precipitation differs and these differences were probably greater in the early Holocene when higher-than-present summer insolation intensified both the subtropical high-pressure system and monsoonal circulation. At that time, summers were drier than present in the regions that receive the majority of annual precipitation in the winter (summer-dry) and wetter in the regions that receive the majority of their annual precipitation in the summer (summer-wet) (Whitlock & Bartlein, 1993). At present, Fairy Lake is located within the summer-wet region, *sensu* Whitlock & Bartlein (1993), receiving more of its precipitation from spring or summer convective storms than winter storms. The ratio of June, July and August (JJA) to December, January, February (DJF) precipitation is 1.34. This is not to say that Fairy Lake receives most of its annual precipitation in June, July, and August—the time of year with the most precipitation is in the springtime, April, May and June (Fig. 2). However, a diverse set of paleoecological research in the NRM and GYE uses the framework of the summer-wet, summer-dry months of JJA and DJF for interpreting regional climate history differences.

For the purposes of comparing the Fairy Lake record with the other records in the NRM and GYE, the months of JJA and DJF will be used in this work.

Vegetation

The Bridger Range has sharply defined lower and upper treelines. On the eastern flank, lower treeline lies at ~1800 m elev, and upper treeline occurs at ~2530 m elev. On the western side, lower treeline is at ~1750 m elev and upper treeline is higher at ~2650

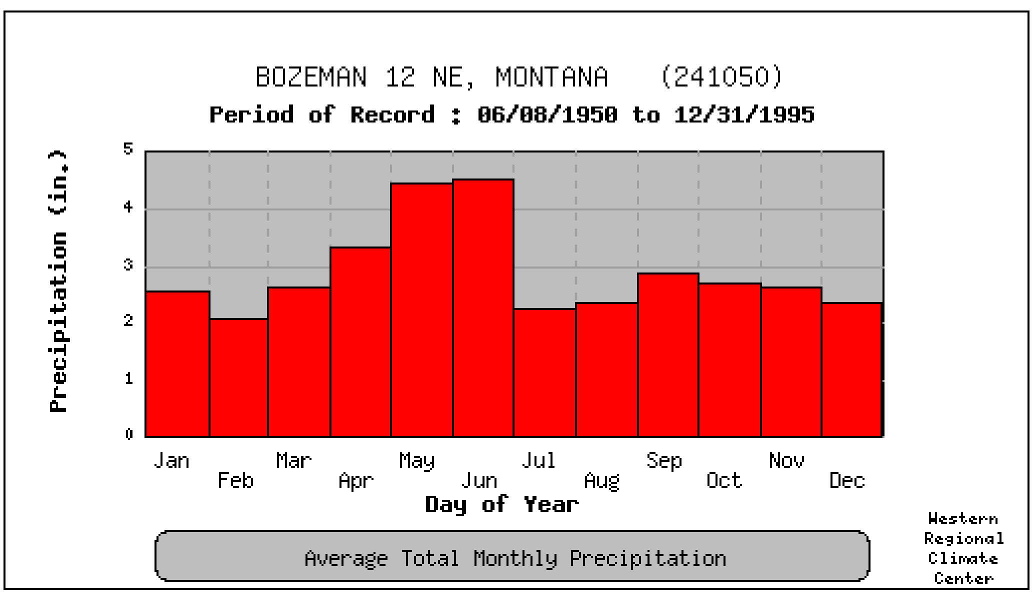

Fig. 2. Annual modern precipitation distribution from the Western Regional Climate Center (Daly et al., 2008, PRISM Climate Group, 2016).

m elev (Fig. 2). Dry open forests at low elevations are composed of *Pinus flexilis* (1219 to 1829 m elev), *Pinus contorta* (1524 to 2290 m elev), and *Pseudotsuga menziesii* (1676 to 2290 m elev), with *Juniperus scopulorum* and *J. communis*. At higher elevations and in mesic settings, forests support *Picea engelmannii* (1737 to 2377 m elev), *Abies lasiocarpa* (2300 to 2400 m elev), *Pinus albicaulis* and *Pinus flexilis* (2200 to 2530 m elev) with *J. communis* (Pfister et al., 1977). Upper treeline consists of krummholz patches of *J. communis*, *P. albicaulis* and *P. flexilis*. The Fairy Lake watershed supports a mixed conifer forest with high-elevation and low-elevation conifers, including *P. albicaulis, A. lasiocarpa, P. engelmannii, P. menziesii, P. contorta, P. flexilis, and J. communis*. At present, *A. lasiocarpa* and *P. engelmannii* are most abundant, but *P. menziesii* is also present as mature trees on south-facing slopes, as well as in the understory near the lake. *P. contorta* and *P. albicaulis* also grow near the lake in smaller numbers. *P. flexilis* and *P. albicaulis* are abundant at higher elevations above the lake. In most cases, *P. flexilis* grows on limestone outcrops at higher elevations, and *P. albicaulis* is found on andesitic deposits (D. Roberts, personal communication, 04/2016, Pfister et al., 1977).

The forest understory supports various shrubs, including *Rosa woodsii*, *Shepherdia canadensis, Amelanchier alnifolia*, *Vaccinium scoparium, Symphiocarpus albus,* as well as diverse herbs. On the immediate west slope of the lake, a large meadow supports *Artemisia tridentata, grass and herbs. Acer glabrum* grows on rocky outcrops. A large meadow also occurs approximately 0.25 km north of Fairy Lake.

Both meadows are covered by grasses, such as *Phleum pretense*, *Agropyron spicatum*, *Festuca idahoensis,* and *Calamogrostis rubescens* as well as *Artemisia*, Asteraceae, and other herbs. *Carex*, *Salix*, and *Equisetum* grow in wet habitats and along the margin of the lake. *Alnus viridis* grows at lower elevation in riparian areas. (Scientific and common names of plant species found in the Fairy Lake Area are provided in Table 1.)

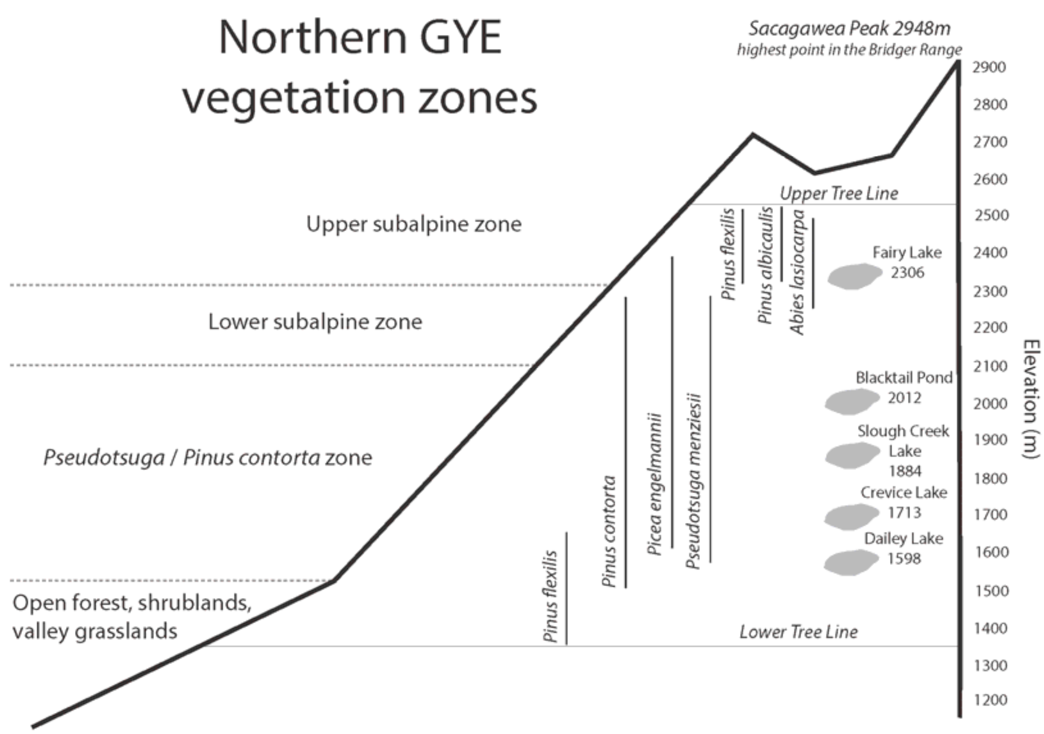

Fig. 3. Generalized vegetation zones for northern GYE, adapted from USDA Forest Service GTR, 1977, Arno, 1980, and Byers et al., 2003. Other sites from the northern GYE are listed at their respective elevations.

The fire regime around Fairy Lake is characterized by infrequent, stand-replacing fires with long intervals (200 years or more) between events (Fischer & Clayton, 1983), although moderate to low-intensity fires likely occurred in conjunction with open Douglas-fir forests.

METHODS

Field

In July 2013 a 10.88-m-long sediment core was obtained in 12 m of water from Fairy Lake using a modified Livingstone square-rod sampler (Wright et al., 1983). The cores were wrapped in plastic, transported back to the Montana State University (MSU) Paleoecology Lab, and stored under refrigeration. In addition, a gravity corer was used to recover the uppermost sediment. The gravity core was extruded in the field at 0.5 cm intervals, and sediment was put into plastic bags.

Lithologic Analysis

Cores were taken to the LacCore National Lacustrine Core Facility at the University of Minnesota, Minneapolis, where they were split and photographed. By use of a Geotek XYZ MSCL logger, magnetic susceptibility was measured in SI units at 0.5 cm intervals. Magnetic susceptibility provides information on mineral clastic input into the lake (Gedye et al., 2000) from erosional events, or from times when the landscape is not comprised of vegetation that can secure said material. For example, an undeveloped landscape following glacial recession.

Table 1. Plants that are currently found in the vicinity of Fairy Lake[1]

Common Name	Terrestrial Plants	Common Name	Terrestrial Plants	Common Name	Aquatic Plants
subalpine fir	*Abies lasiocarpa*	common red paintbrush	*Castilleja miniata*	wire rush	*Juncus arcticus*
Engelmann spruce	*Picea engelmannii*	spotted water hemlock	*Cicuta maculata*	sedges	Cyperaceae
whitebark pine	*Pinus albicaulis*	Hooker's thistle	*Cirsium hookerianum*	willows	*Salix spp.*
lodgepole pine	*Pinus contorta*	sedge	Cyperaceae	horsetails	*Equisetum spp.*
limber pine	*Pinus flexilis*	tall mountain larkspur	*Delphinium occidentale*	saxifrages	Saxifrageaecea
Douglas-fir	*Pseudotsuga menziesii*	fireweed	*Epilobium angustifolium*		
common juniper	*Juniperus communis*	cushion buckwheat	*Eriogonum ovalifolium*		
Rocky Mountain maple	*Acer glabrum*	Idaho fescue	*Festuca idahoensis*		
serviceberry	*Amelanchier alnifolia*	green gentian	*Frasera speciosa*		
prairie sagewort	*Artemisia frigida*	sweet-scented bedstraw	*Galium triflorum*		
big sagebrush	*Artemisia tridentata*	brown-eyed Susan	*Gaillardia aristata*		
creeping Orgeon-grape	*Berberis repens*	geranium	*Geranium spp.*		
Utah honeysuckle	*Lonicera utahensis*	western rattlesnake plantain	*Goodyera oblongifolia*		
mallow ninebark	*Physocarpus malvaceus*	sunflower	*Helianthella ssp.*		
squaw currant	*Ribes cereum*	silvery lupine	*Lupinus argenteus*		
prairie rose	*Rosa woodsii*	bluebell	*Mertensia spp.*		
thimbleberry	*Rubus parviflorus*	western blue flax	*Linum lewisii*		
willow	*Salix spp.*	mountain sweet-cicely	*Osmorhiza chilensis*		
Canada buffaloberry	*Shepherdia canadensis*	penstemon	*Penstemon spp.*		
western mountain-ash	*Sorbus scopulina*	field timothy	*Phleum pratense*		
common snowberry	*Symphiocarpus albus*	cinquefoil	*Potentilla spp.*		
mountain huckleberry	*Vaccinium globulare*	dwarf raspberry	*Rubus arcticus*		
whortleberry	*Vaccinium scoparium*	western rayless coneflower	*Rudbekia occidentalis*		
baneberry	*Actaea rubra*	arrow-leaved groundsel	*Senecio triangularis*		
yarrow	*Achillea millefolium*	birch-leaved spiraea	*Spiraea betulifolia*		
short-beaked agroseris	*Agoseris glauca*	common dandelion	*Taraxacum officinale*		
broad-glumed wheatgrass	*Agropyron spicatum*	meadow rue	*Thalictrum occidentale*		
nodding onion	*Allium cernuum*	clover	*Trifolium ssp.*		
wild chive	*Allium schoenoprasum*	hellebore	*Veratrum viride*		
anemone	*Anemone spp.*	voilet	*Viola spp.*		
rosy pussytoes	*Antennaria microphylla*	mountain death-camas	*Zigandenus elegans*		
yellow columbine	*Aquilegia flavescens*				
Rocky Mountain columbine	*Aquilegia saximontana*				
heart-leaf Arnica	*Arnica cordifolia*				
ballhead sandwort	*Arenaria congesta*				
milk-vetch	*Astragalus spp.*				
buckley pinegrass	*Calamagrostis rubescens*				
common harebell	*Campanula rotundifolia*				

1. *Scientific nomenclature follows Dorn, 1984, & Kershaw et al., 1998.*

A Geotek MSCL-S was used to measure core sediment density (grams cm^{-3}), and photograph the cores. Additional lithologic descriptions were undertaken in the MSU Paleoecology Lab. Samples of 1 cm^3 were taken at 8-cm intervals and used for loss-on-ignition (LOI) analysis to determine the organic and carbonate content of the sediment (Dean, 1974). Samples were dried for 24 hours at 80°C to remove water. They were then placed in a muffled furnace for 2 hours at 550°C to remove organic material. Afterward, they were burned again for 2 hours at 900°C to remove inorganic carbonates. Weight loss after each burning was used to determine the percent of organic and carbonate content. The organic or inorganic content of the samples reveal changes in lake productivity.

Table 2. Radiocarbon samples for Fairy Lake.

Depth (cm)	Uncalibrated ^{14}C age	Calibrated age range (cal yr BP)	Material Dated	Lab number / reference
75.5	1270 ± 20	677 – 881	Plant debris	NOSAMS
121.5	1820 ± 20	1305 – 1559	Plant debris	NOSAMS
178.0	2250 ± 20	2406 – 2638	Plant debris	NOSAMS
205.0	2710 ± 25	3093 – 3320	*Picea* needle	NOSAMS
270.0	4610 ± 30	5143 – 5518	Plant debris	NOSAMS
302.0	5350 ± 30	6308 – 6860	Plant debris	NOSAMS
333.0		7537 – 7728	Mazama Ash	Egan et al., 2015
365.5	9030 ± 40	8741 – 9721	Plant debris	NOSAMS
477.0	11,600 ± 50	13,300 – 13,616	Glacier Peak Ash	Kuehn et al., 2009

Chronology

The chronology of the Fairy Lake core was based on AMS ^{14}C dating of seven terrestrial plant macrofossils and the age of two known tephras: Mount Mazama, 7633 cal yr BP +/- 49 (Egan et al., 2015) and Glacier Peak 13,599 ^{14}C yr BP +/- 95 (Kuehn et al., 2009) (Table 2, Fig. 3). ^{14}C dates were converted to calendar years using CLAM software version 2.2 in R and an age-model was developed (smoothing spline type 4, with spar = .5, IntCal13, Blaauw, 2010, Reimer et al., 2013). Bayesian ACcumulatiON histories for deposits, using BACON software, was also considered in developing the chronology. BACON calculates a probability density function for the age of each sample level. It also estimates the median and weighted mean ages, which are useful for plotting stratigraphic diagrams.

However, the probability that these ages were the real ages is small, because these ages are not derived from a smoothing function, such as a polynomial or spline. As a result, BACON produces ages that have highly variable centimeter-to-centimeter differences, which are unrealistic and consequently not appropriate for estimating flux values. CLAM, on the other hand, fits a large number of smoothing functions to produce a smooth curve for the median sample ages. For that reason, CLAM was used to develop the age model for the Fairy Lake core.

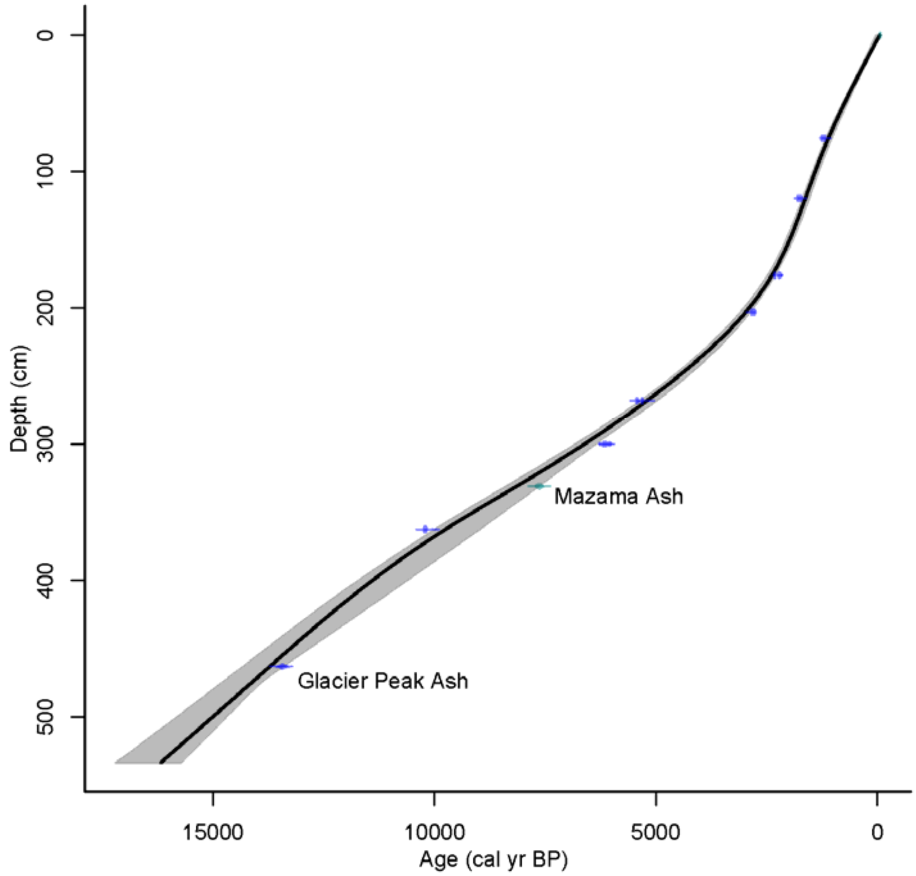

Fig. 4. Age-depth model for Fairy Lake. Dots represent calibrated radiocarbon dates and tephra are identified. Horizontal bars on dots show median 2 sigma standard deviation around each age determination. Solid black line is the interpolated age for each depth in the core. Grey area represents a 95% confidence interval relative to those ages. The age of the Mazama Ash was entered into the model as a calibrated date (*Egan et al.,* 2015). Clam 2.2 was used in R to create this model (http://chrono.qub.ac.uk/blaauw/clam.html, https://www.r-project.org).

Pollen Analysis

Samples of 0.5 cm^3 for pollen analysis were taken at 4-cm intervals. Procedures outlined in Bennett & Willis (2001) were used to process pollen samples. Pollen grains were identified at magnifications of 400X and 1000X on a Nikon Eclipse 50i compound microscope, and 300 – 350 terrestrial pollen grains were counted per sample. Pollen percentages were calculated by dividing the individual pollen count against total terrestrial grains counted. Pollen concentration (grains cm^{-3}) was calculated by adding a known concentration of *Lycopodium* tracer to each sample (Bennett & Willis, 2001). Pollen accumulation rates (PAR; grains cm^{-2} yr^{-1}) were calculated by dividing the pollen concentration by sediment deposition rate of that sample (Bennett & Willis, 2001).

Pollen grains were identified using the reference collection housed at the MSU Paleoecology Lab, as well as pollen identification keys and atlases (e.g., Kapp et al., 2000, Moore et al., 1978, McAndrews et al., 1973). *Pinus* subg. *Strobus* pollen in this region includes *P. albicaulis and P. flexilis* and is identified by the presence of verrucae on the distal membrane between the bladders. We refer to this pollen type as *Pinus flexilis*/*albicaulis*. *Pinus* subg. *Pinus* pollen was dominantly from *P. contorta*, although *P. ponderosa* may have also contributed to this pollen type. It is identified by the absence of verrucae on the distal membrane. *P. ponderosa* grows at low elevations in the region but does not occur in the Bridger Range at present. Hence, we refer to the pollen type as *Pinus contorta*-type. *Pinus* pollen grains that were damaged or had missing distal membranes were classified as *Pinus undifferentiated*.

Pseudotsuga and *Larix* pollen grains are nearly indistinguishable (Gugger & Sugita, 2010). At present, *Larix* does not grow in the Bridger Range, but *L. occidentalis* and *L. lyallii* occur on the west side of the Continental Divide in northwestern Montana. This pollen type was referred to as *Pseudotsuga/Larix* at Fairy Lake. *Juniperus*-type pollen is from *J. communis*, *J. scopulorum*, and possibly *J. horizontalis*. *Alnus* pollen probably comes from *A. viridis*. The category "Total Rosaceae" includes Rosaceae undifferentiated, *Amelanchier*-type, *Spiraea*-type, and *Prunus*-type. "Other Amaranthaceae" refers to taxa in the family other than *Sarcobatus vermiculatus*. The category "Total Pteridophytes" consists of spores that did not have a discernable stratigraphic trend, and include *Dryopteris* and *Pteridium* spore types. The category "Other Herbs" includes taxa that also had no discernable trend, *Ceanothus, Cornus, Arceuthobium,* Asteraceae subfield Cichoroideae, *Polygonum,* Brassicaceae, *Bidens*-type, *Ephedra, Galium,* Onagraceae, Ranunculaceae, Caryophyllaceae, Fabaceae, *Rumex*, Apiaceae, *Selaginella densa-type*, and *Thalictrum*. Pollen grains that were damaged, hidden or corroded beyond identification were classified as Indeterminate, and grains that could not be identified with the available reference material were classified as Unknown. These were included in the terrestrial sum. Aquatic taxa with no distinctive stratigraphy were grouped into a category called "Total Aquatics" that included *Myriophyllum, Equisetum, Utricularia,* and *Typha latifolia*.

Charcoal Analysis

Samples of 2 cm^3 were taken at 0.5 cm intervals and used for charcoal analysis. The samples were soaked in sodium hexametaphosphate and bleach for 24 hours and then rinsed through a 125-µm-mesh sieve. Charcoal particles were counted with a Nikon SMZ800 stereoscopic microscope using procedures outlined in Whitlock & Larsen (2001). Charcoal accumulation rates (CHAR, particles cm^{-2} yr^{-1}) were calculated by dividing the charcoal concentration by the deposition rate of each sample. CharAnalysis software (https://sites.google.com/site/charanalysis/) was used to decompose the CHAR record into a slowly varying component (background CHAR= BCHAR) and statistically significant peaks component (peaks that meet a user-defined threshold for fires). BCHAR is the low-frequency trend of CHAR, and is generally considered to be a record of area burned or biomass burning within a 20-25 km radius of the site (Higuera et al., 2009, Higuera et al., 2010). The peaks represent individual fire episodes (i.e., one or more fires occurring within the sampling interval) within 1-3 km radius of the lake (Higuera et al., 2009, Higuera et al., 2010).

To identify BCHAR, a 750-yr lowess smoother that was robust to outliers was applied to the CHAR time series. A 750-yr window was chosen because these results produced the highest signal-to-noise ratio. To detect significant charcoal peaks, a user-determined threshold value (peaks with <3 signal-to-noise index) was selected to identify fire episodes. Those peaks were examined in a Poisson distribution to determine if they had a >5% probability of coming from the same distribution. If they had >5%, they were discarded as false or redundant peaks. Fire return intervals (yr $fire^{-1}$) were calculated as the years between fire peaks. Peak magnitude was measured as pieces cm^{-2} $peak^{-1}$. A 1000-yr smoothing window was implemented to calculate fire-episode frequencies (fires 1000 yr^{-1}).

RESULTS

Lithology

The core lithology was divided into two primary units (Fig. 5): Unit 1 (500 – 351 cm depth) was composed of gray and pink clay with red bands of clay. The bottom of the core had a large (~40cm) red clay deposit, and most of the red clay layers are near the bottom of this unit. This unit terminated with a thick (3 cm) red layer. The percent of organic content ranged from 3-14%, and the carbonate content ranged from 2-27%. Magnetic susceptibility ranged from 1.1-128.4 SI units, with higher values deeper in this unit.

A tephra layer was identified at 427 cm depth, and based on the age model and other records in the region, it was inferred to be Glacier Peak ash, which erupted at 13,599 +/- 95 cal yr BP (Kuehn et al., 2009). Unit 2 (350 – 0 cm depth was composed of dark brown fine-detritus gyttja with irregularly spaced red clay layers that were more frequent between 170 and 60 cm depth. The organic content ranged from 7-42%, and the carbonate content was between 2-20%. Magnetic susceptibility ranged from 0-36.6 (SI units). A tephra layer was identified at 283 cm depth and attributed to the Mount Mazama eruption in southwestern Oregon, which occurred at 7633 +/- 49 cal yr BP (Egan et al., 2015). The carbonate content in this unit is higher overall than in Unit 1. In particular, from a depth of 275 to 150 cm, the carbonate content was increased from

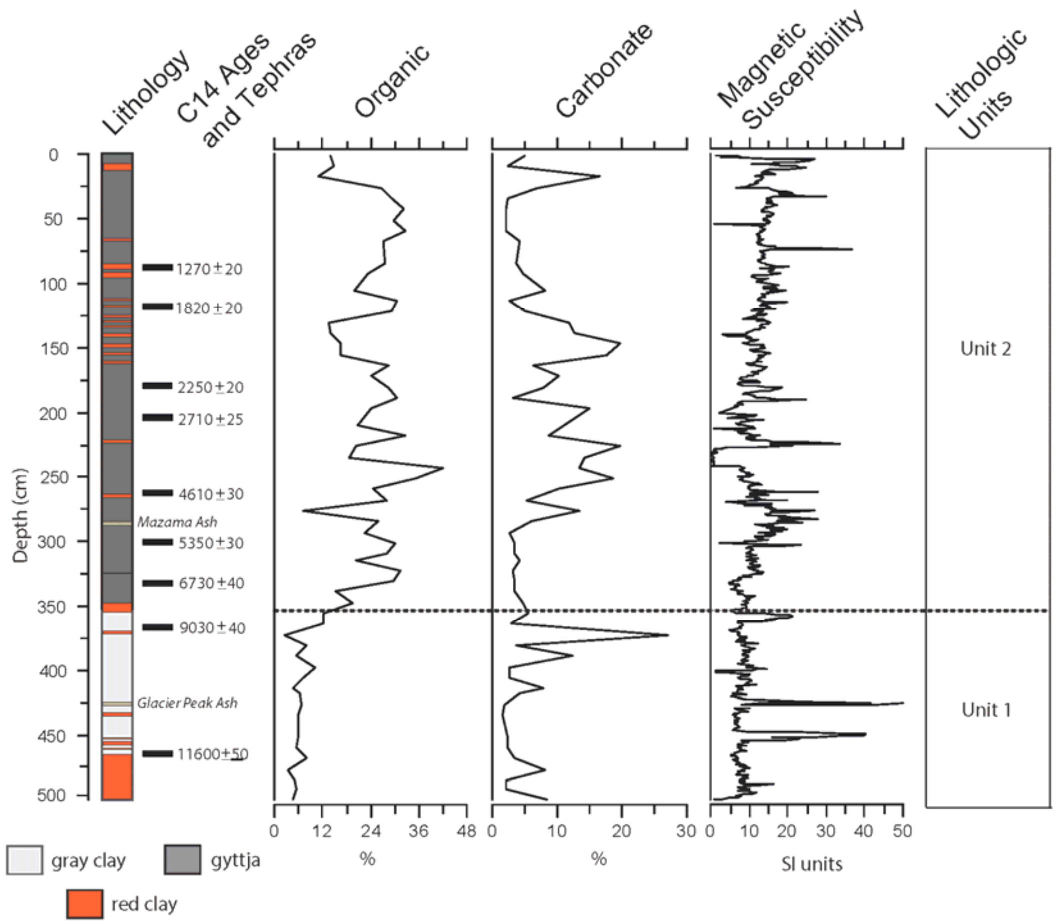

Fig. 5. Lithology, radiocarbon and tephra locations, organic and inorganic content of the core, magnetic susceptibility, and unit divisions of the Fairy Lake core.

previous and immediately following. The elevated levels of carbonate might be the result of lower lake level and/or increased temperatures. Increases in inorganic carbon are often the result of increased temperatures, lake stratification, increases in pH of the water, and/or algal photosynthesis.

Pollen and Charcoal

The three pollen zones were identified using CONISS cluster analysis (Fig. 6) (Grimm, 1988).

Zone FL-1 (ca. 15,400 cal yr BP – 11,400 cal yr BP, 500 – 350 cm depth)

Total *Pinus* was 7-67% in this zone. *Pinus contorta*-type percentages ranged from 1 to 15%. *Pinus albicaulis/flexilis* percentages peaked (34%) at ca. 13,700 cal yr BP and then decreased to between 3 and 15%. *Picea* and *Abies* values were low in this zone, ranging from 1-6%. *Pseudotsuga/Larix* pollen was absent until ca. 12,900 cal yr BP. Pollen of *Juniperus*-type, *Alnus, Betula, Salix, Populus*, and Total Rosaceae were each present at values of 2-5%, with high percentages before ca. 14,000 cal yr BP. *Sarcobatus* pollen was present at values of ~3% at ca. 15,400 cal yr BP, but mostly present at <3%. Poaceae percentages were 2-10% with a peak of 13% at ca. 15,200 cal yr BP. Cyperaceae percentages reached 5% at ca. 15,400 and 12,400 cal yr BP but had values of <3% for most of the zone. *Artemisia* percentages were 30-49% in the beginning of the zone, increased to 53% at ca. 12,400 cal yr BP, and decreased to 35% toward the top of this zone. Asteraceae sub. Asteroideae pollen had values of <2% throughout the zone. Other Amaranthaceae accounted for <2% through most of the zone and increased to 9% at ca. 12,400 cal yr BP. *Ambrosia*-type, Other Herbs and Total Pteridophytes were present at <2% each as were Other Aquatics. Pollen accumulation rates (PARs) ranged from 353 to 1024 grains $cm^{-2}\ yr^{-1}$, which is typical of modern dwarf-shrub tundra (Davis et al., 1973).

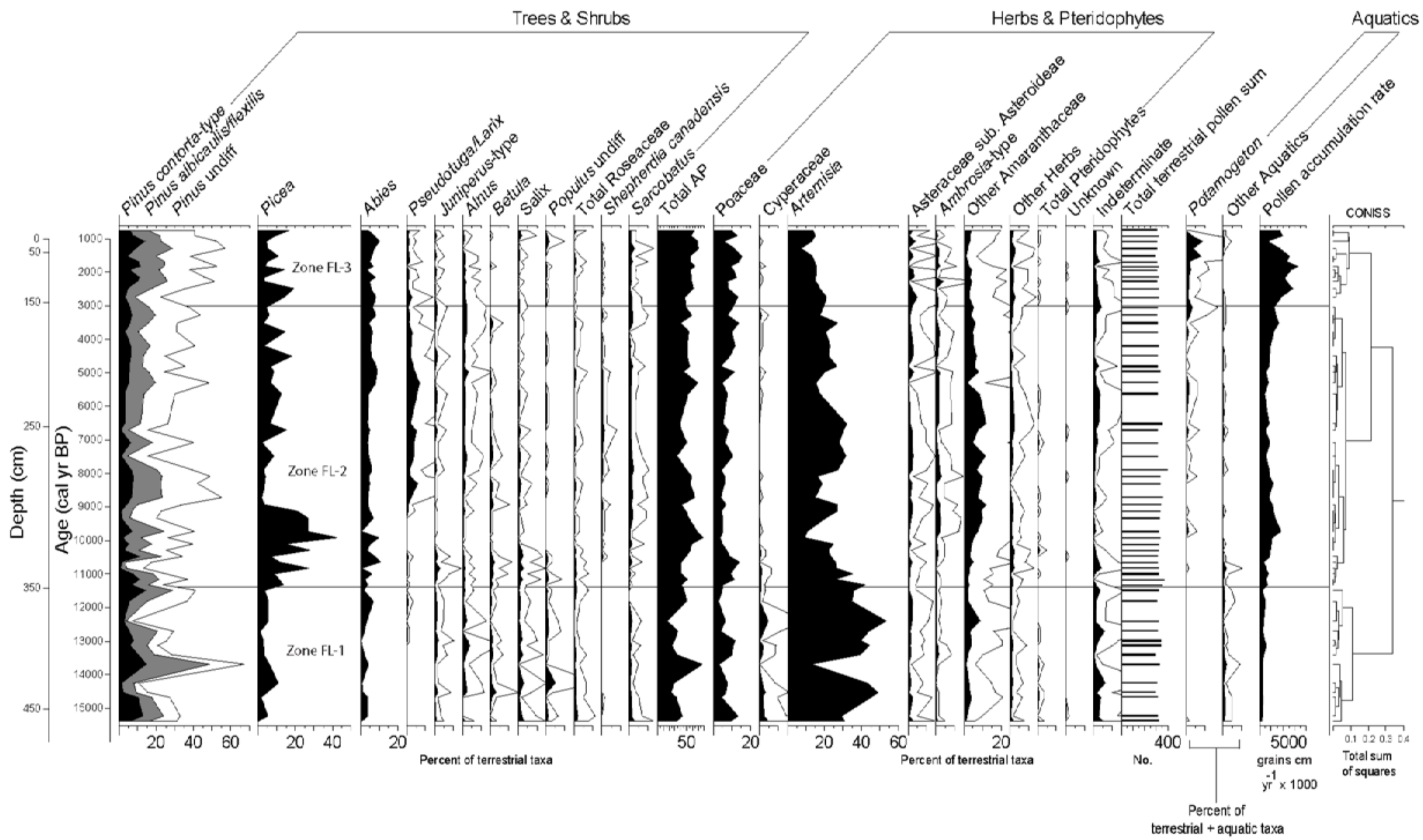

Fig. 6. Pollen percentage diagram showing selected taxa from Fairy Lake

Based on modern pollen data from the GYE, high percentages (53%) of *Artemisia*, Poaceae and Cyperaceae pollen, along with *Selaginella densa*, suggest an open, tundra-steppe (Whitlock, 1993, Fall, 1994). Background charcoal levels (BCHAR) were low (0.001-.004 particles cm^{-2} yr^{-1}), but rose slightly after 12,500 cal yr BP, and fire frequencies were <4 episodes 1000 yr^{--1} (Fig. 7), both of which suggest limited fire activity.

Zone FL-2 (ca. 11,400 cal yr BP – 3000 cal yr BP, ~350 – 150 cm depth)

Total *Pinus* percentages ranged from 12 to 55% in this zone. *Pinus contorta*-type percentages ranged from 5 to 11% with highest values at ca. 11,200 cal yr BP. *Pinus albicaulis/flexilis* ranged from 2 to 17%, with highest percentages at ca. 9700 cal yr BP. *Picea* increased to 42% at ca. 9900 cal yr BP and decreased to 3-17% for the remainder of the zone. *Abies* values were between 3 and 11%. *Pseudotsuga/Larix* increased from <1 to 6% at ca. 8900, with peaks at ca. 8300, 6700, 5300 cal yr BP. Pollen of *Juniperus*-type, *Alnus, Betula, Salix, Populus*, and Total Rosaceae were present at 1-3% at the base of the zone, and then mostly disappeared from the record after ca. 10,400 cal yr BP. *Alnus* and *Salix* increased slightly at ca. 11,400 – 10,000 cal yr BP as well as at ca. 9000 cal yr BP and ranged from 0.5-2.5%. *Shepherdia canadensis* and *Sarcobatus* were present in values of <2%. Percentages of Poaceae pollen had values of 4-13%, and those of Cyperaceae were low (<2%). *Artemisia* percentages were initially high at 42%, and decreased to 10% at ca. 9900 cal yr BP, and then ranged between 15-30% for the rest of the zone.

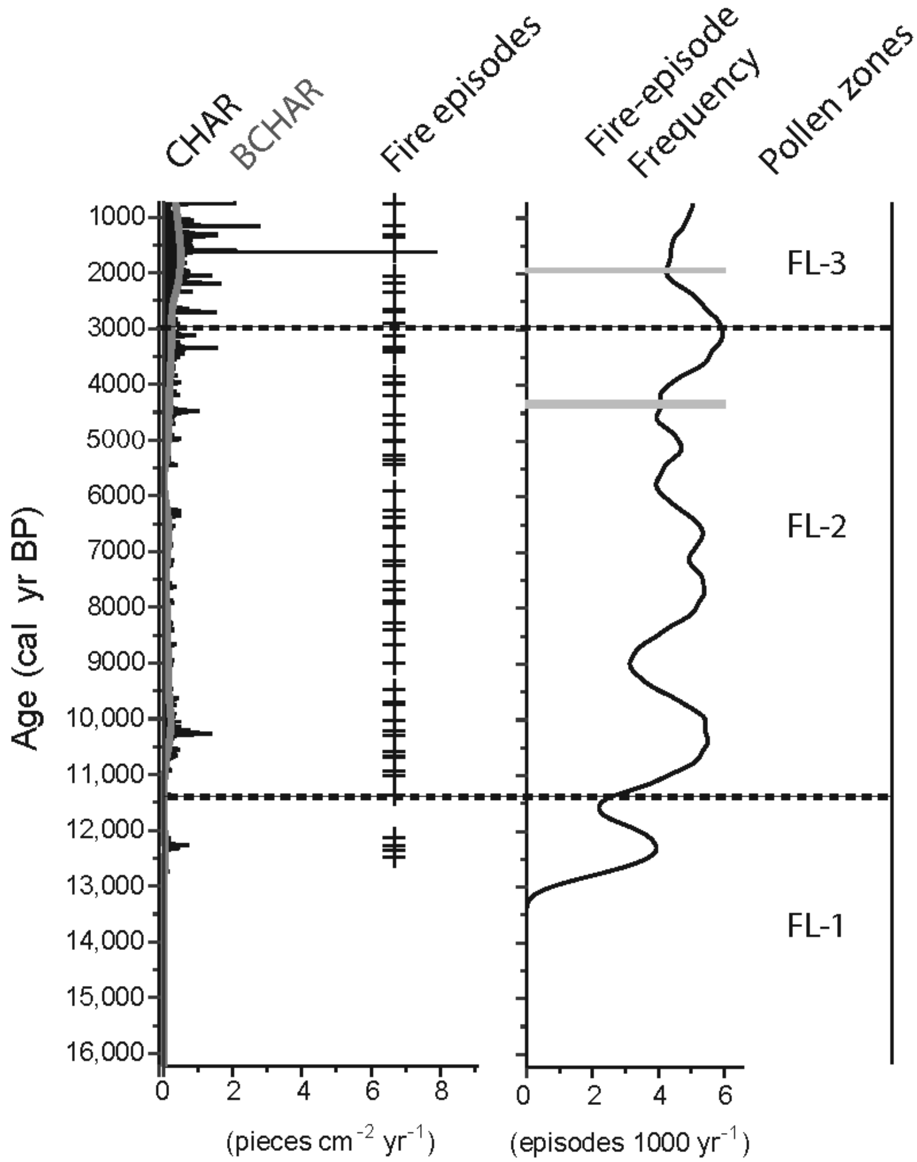

Fig. 7. Charcoal data and associated pollen zones from Fairy Lake.

Pollen of Asteraceae sub. Asteroideae were present in values <3%. *Ambrosia*-type were <2%, Other Amaranthaceae were 2-12%, and Other Herbs were <2.5%. Total Pteridophytes and Other Aquatic types were present in low amounts (<2%). PARs ranged from 732-3590 grains cm^{-2} yr^{-1}, which is characteristic of modern forest-tundra vegetation (Davis et al., 1973).

High percentages of *Picea,* Asteraceae sub. Asteroideae, Other Amaranthaceae, *Ambrosia*-type, Poaceae, and Other Herbs suggest the presence of a spruce parkland from ca. 11,400 – 9100 cal yr BP (Whitlock, 1993, Fall, 1994). This vegetation was replaced by an open forest of *Pinus, Picea* and *Abies* at ca. 9000 cal yr BP. *Pseudotsuga* was increasing, likely at lower elevations, from ca. 9100 to 8300 cal yr BP, when it increased and maintained relatively high percentages, increasing to 7% at ca. 5300 cal yr BP. Pollen of herbaceous taxa remain high throughout this zone, with higher periods from ca. 11,000 – 10,000 cal yr BP and from ca. 8000 – 4000 cal yr BP. Other Amaranthaceae increase from ca. 10,500 to ca. 3000 cal yr BP. BCHAR in this zone was low (0.01-0.2 particles cm^{-2} yr^{-1}), and fire-episode frequency was generally higher than the previous zone (2-6 episodes 1000 yr^{-1}). Fires were frequent, but not stand replacing, as evidenced by the low levels of BCHAR.

Zone FL-3 (ca. 3000 cal yr BP – 745 cal yr BP, 150 – 0 cm depth)

Total *Pinus* percentages ranged from 22-56% with *Pinus contorta*-type at 4-14%, and *Pinus albicaulis/flexilis* at 5-20%. Pollen of *Picea* ranged from 3-19%, and that of *Abies* was present at values of 4-10%. Pollen of *Pseudotsuga/Larix* accounted for <3%. Values of *Juniperus*-type, *Alnus, Betula, Salix, Populus* Undiff. and Total Rosaceae were <2%, and *Sarcobatus* was <3%. Poaceae percentages ranged between 6 and 15%, and values of Cyperaceae were <1%. *Artemisia* percentages ranged from 7-21%, Asteraceae sub. Asteroideae, Other Amaranthaceae, and *Ambrosia*-type were present in values of <5%. Percentages of Other Herbs were <3%, Total Pteridophytes were <1%, and *Potamogeton* were 2-9%. PARs were from 1342-5625 grains cm^{-2} yr^{-1}, consistent with values from modern forest-tundra vegetation (Davis et al., 1973)

Based on modern pollen samples, this zone marks the establishment of a closed forest, dominated by *Pinus, Picea* and *Abies* and a component of *Pseudotsuga* (Fall, 1994). BCHAR values for this zone were highest in this zone (0.2-0.5 particles cm^{-2} yr^{-1}), and fire-episode frequency ranged between 4 and 6 episodes 1000 yr^{-1}. The modern forest fire regime for this type of forest is severe stand replacing fires with some moderate to low-intensity fires (Fischer & Clayton, 1983).

DISCUSSION

Vegetation and Fire History of the Fairy Lake Area

The pollen, charcoal, and lithologic records from Fairy Lake offer new information on the vegetation, fire, and climate history of the Bridger Range. This reconstruction was compared with nearby records to gain an understanding of the environmental history of the GYE and NRM. Paleoclimate model simulations provide independent information about the regional climate changes that occurred over the course of the record (Whitlock & Bartlein, 1993, Bartlein et al., 1998). Other sites within the northern GYE are Crevice Lake, Dailey Lake, Blacktail Pond and Slough Creek Lake. For more information on these lakes, refer to Table 3. The discussion is divided into four periods—the late-glacial (ca. 15,000 – 10,500 cal yr BP), early Holocene (ca. 10,500 – 7100 cal yr BP), middle Holocene (ca. 7100 – 3000 cal yr BP), and late Holocene (ca. 3000 – 745 cal yr BP).

Late-glacial Period (ca. 15,500 to 10,500 cal yr BP)

Fairy Lake was likely first free of ice at ca. 15,500 cal yr BP (K. Pierce, personal communication, 09/2015). The initial vegetation, tundra-steppe, featured high levels of *Artemisia* and abundant herbaceous taxa at Fairy Lake and other sites in the northern GYE and suggests that the landscape was largely treeless and dominated by sagebrush and grasses. Shrubs, such as *Alnus, Betula* and *Salix* were first present at ca. 14,500 cal yr BP and likely colonized riparian areas on the deglaciated landscape. *Juniperus* was also present at ca. 14,500 cal yr BP and probably grew on glacial till and other well-drained substrates, based on its modern distribution (Whitlock, 1993). A small increase in *Pinus albicaulis*-type pollen ca. 13,800 cal yr BP indicates the presence of *P. albicaulis* or *P. flexilis*, possibly at the lower elevations in the valley or in low numbers near Fairy Lake.

Blacktail Pond also recorded moderate levels (38%) of *Pinus albicaulis*-type pollen between 13,000 and 12,000 cal yr BP (Huerta et al., 2009). Pollen of aquatics (e.g., *Myriophyllum, Equisetum*) were abundant at Fairy Lake in the late-glacial period and suggest shallow water and wetland habitats. By ca. 11,500 cal yr BP, rising pollen levels of *Picea* and *Pinus albicaulis*-type and *Pinus contra*-type indicate increasing moisture and a landscape transition from early tundra-steppe to more forest. Fires were rare prior to ca. 12,500 cal yr BP, but with the presence of trees and woodier biomass, fire frequency increased from 0 to 4 episodes 1000 yr^{-1}.

The pollen data suggest cool, dry conditions during the late-glacial period, with increasing temperature and moisture after 12,500 cal yr BP. Paleoclimate model simulations for this time period show that temperatures were higher than the full-glacial period but cooler than at present, and levels of effective moisture were low but increasing (Bartlein et al., 1998). Progressively warmer and moister conditions were likely a response to higher summer insolation and a northward shift of the jet stream (Whitlock &

Table 3. Information about study sites discussed in text. Sites are arranged by approximate west to east transect.

Site Name	Latitude / Longitude	Elevation (m)	Reference	Modern vegetation	Modern precipitation (JJA/DJF)[1](cm)
Burnt Knob Lake	45.700 N / 114.990 W	2250	*Brunelle et al.* (2003)	*Abies* and *Pinus albicaulis* forest	.58
Hoodoo Lake	46.320 N / 114.652 W	1770	*Brunelle et al.* (2005)	*Pinus contorta, Picea* forest with some *Abies*	.41
Baker Lake	45.892 N / 114.262 W	2300	*Brunelle et al.* (2005)	*Pinus albicaulis, Larix lyallii, Abies, Picea* forest	.96
Pintlar Lake	45.841 N / 113.440 W	1921	*Brunelle et al.* (2005)	*Pinus contorta, Pseudotsuga,* some *Picea* forest	2.8
Fairy Lake	45.904 N / 110.958 W	2306	*This study*	*Picea, Abies, Pinus albicaulis/flexilis* forest	1.3
Dailey Lake	45.262 N / 110.815 W	1598	*Krause et al.* (2015)	Grassland and *Artemisia* steppe	3.3
Crevice Lake	45.000 N / 110.578 W	1713	*Whitlock et al.* (2007)	*Pseudotsuga, Juniperus, Pinus flexilis, Artemisia* forest	2.8
Blacktail Pond	44.955 N / 110.602 W	2012	*Huerta et al.* (2009), *Krause & Whitlock* (2013)	*Artemisia* steppe, with nearby *Pseudotsuga*	1.7
Slough Creek Lake	44.930 N / 110.352 W	1884	*Millspaugh et al.* (2004)	*Pseudotsuga* parkland	1.5
Cygnet Lake	44.660 N / 110.620 W	2530	*Millspaugh et al.* (2000)	*Pinus contorta* forest	1
Floating Island Lake	44.550 N / 107.467 W	2609	*Burkart* (1976)	Mixed conifer forest, with *Juniperus*	1.8
Beaver Lake	44.179 N / 107.260 W	2561	*Burkart* (1976)	Mixed conifer forest, with *Juniperus*	2.1
Sherd Lake	44.269 N / 107.012 W	2665	*Burkart* (1976)	Mixed conifer forest, some *Artemisia*	3.4

[1]Average precipitation for June, July, and August was summed and divided by summed average precipitation for December, January and February for the period from 1894 to 2016 (PRISM climate data, 2016).

Bartlein, 1993). The lithology of the core at this time also supports a sparsely vegetated landscape; mostly clays are deposited with little organic material (Fig. 5).

Other paleoecological records in northern GYE show a shrub-dominated landscape with few trees in the first millennia following glacial recession from ca. 15,000 to 13,000 cal yr BP (Fig. 8)(e.g., Krause et al., 2015). As conditions became wetter and warmer after ca. 12,500 cal yr BP, the landscape supported *Salix, Betula, Alnus, Juniperus* and herbs (Millspaugh et al., 2004, Krause et al., 2015, Krause & Whitlock, 2013). The landscape was, at first, sparsely vegetated with discontinuous shrub cover, and then progressively became more vegetated. The $\delta^{18}O$ record from Blacktail Pond in the northern GYE indicates cooler conditions early in the late-glacial period followed by warming toward the end of the period, ca. 11,500 cal yr BP (Krause & Whitlock, 2013). Increasing winter moisture in the GYE at this time is attributed to a northward shift of storm track position following continental ice sheet recession (Bartlein et al., 1998, Licciardi & Pierce, 2008).

The Younger Dryas Chronozone (YDC; 12,900 – 11,500 cal yr BP (Alley, 2000)) is not registered as a distinctive event at Fairy Lake, but ice advances in the Wind River Range at this time suggest a short reversal to cold conditions (Gosse et al., 1995). In the Canadian Rocky Mountains, concurrent ice advances are also attributed to cooling during the YDC (Reasoner et al., 1994). Although it is possible that YDC had climate impacts in the Fairy Lake area, it is not immediately evident in the pollen or charcoal record.

The establishment of a subalpine parkland of *Picea* and *Pinus albicaulis* or *P. flexilis* at ca. 11,300 cal yr BP is later at Fairy Lake than at other places in the northern GYE. *Picea* parkland developed at Dailey Lake at ca. 13,300 cal yr BP (Krause et al., 2015), at Blacktail Pond at ca. 12,900 cal yr BP (Krause & Whitlock, 2013), and at Slough Creek Lake at ca. 12,000 cal yr BP (Millspaugh et al., 2004). The late establishment of spruce at Fairy Lake could be a result of the lake's higher elevation, or it could imply that *Picea* expanded south into the Paradise Valley and YNP before expanding north into the Bridger Range. *Picea* parkland persists at Fairy Lake until ca.

9000 cal yr BP. In contrast, the pollen data at Dailey Lake suggest that *Picea* parkland was replaced there by closed forest of *Picea, Abies, and Pinus albicaulis*-type by ca. 12,300 cal yr BP. *Picea* pollen declined and that of *Pinus contorta*-type increased at Blacktail Pond, indicating a closed subalpine forest at 11,350 cal yr BP (Krause & Whitlock, 2013), and high *Picea* values were replaced by rising *Pinus* and *Juniperus* percentages at 11,000 cal yr BP at Slough Creek Lake, marking establishment of a mixed forest of *Pinus contorta*, *Pinus-albicaulis*-type, and *Juniperus* (Millspaugh et al., 2004).

The vegetation lag at Fairy Lake in shifting to Picea and *Pinus albicaulis* or *P. flexilis* parkland implies environmental conditions at sites to the south of Fairy Lake were more suitable (e.g. warmer) for earlier expansion of closed and mixed conifer forests. This delay may be attributed to Fairy Lake's high elevation relative to the other sites in the northern GYE.

Early-Holocene Period (ca. 10,500 to 7100 cal yr BP).

The decline of *Picea* pollen at Fairy Lake coincided with an increase in *Pinus albicaulis*/*flexilis*, *Pinus contorta*-type, *Pinus*, and *Pseudotsuga/Larix*, as well as a slight increase in *Abies,* indicating an open forest of *P. albicaulis* or *P. flexilis* with lesser amounts of *P. contorta*, *Abies*, and *Picea. Pseudotsuga* may also have been present. Increases in *Betula, Alnus* and *Salix* indicate a period of rising temperatures and increasing moisture levels. *Sarcobatus* and Other Amaranthaceae, *Ambrosia*-type, and Asteraceae sub. Asteroideae increased at ca. 10,000 cal yr BP, which suggests lowland

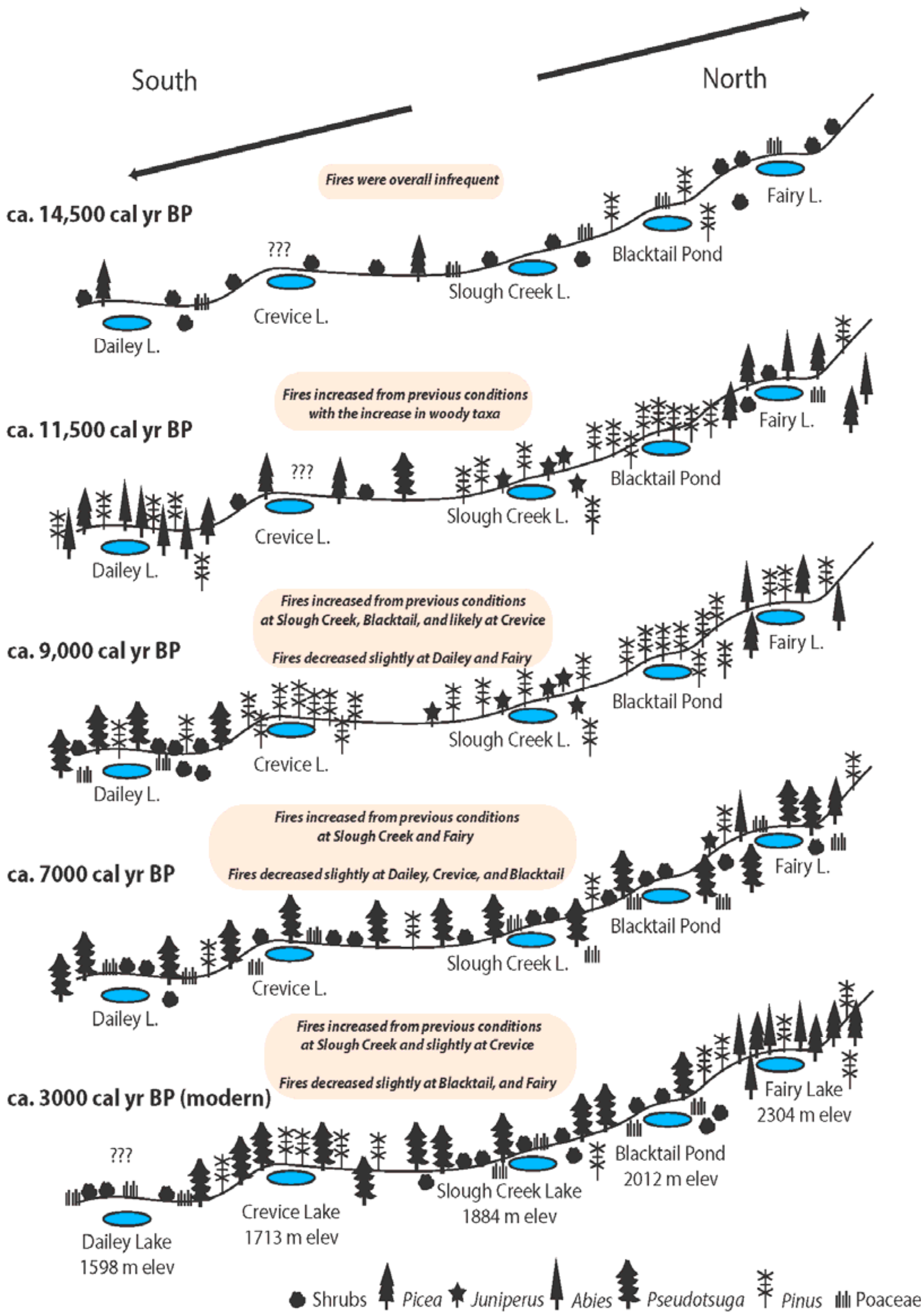

Fig. 8. Schematic diagram showing vegetation and fire history at different time periods, based on an elevational transect of sites in the northern GYE.

steppe expansion in response to rising temperatures. *Sarcobatus* pollen likely comes from *Sarcobatus vermiculatus* on dry sites east of the Bridger Range. Dailey Lake transitioned from a closed mixed conifer forest to a mixture parkland of *Artemisia* steppe and *Pseudotsuga* and *Pinus contorta* forest at 10,200 cal yr BP (Krause et al., 2015). Blacktail Pond area supported closed forest, dominated by *Pinus contorta* from 11,350 until ca. 8200 cal yr BP, when *Pseudotsuga* parkland developed (Krause & Whitlock, 2013). Crevice Lake was surrounded by a closed *Pinus* forest, either *P. albicaulis* or *P. flexilis*, until ca. 8200 cal yr BP, and increasing *Pseudotsuga*/*Larix* and Poaceae percentages indicate establishment of *Pseudotsuga* parkland at ca. 8000 cal yr BP (Whitlock et al., 2012). The area around Slough Creek Lake supported a mixed forest of *Pinus* and *Juniperus* during the early Holocene (Millspaugh et al., 2004).

Fires in the early Holocene at Fairy Lake rose to 5 episodes 1000 $yr^{-1}$and BCHAR levels increased from previously low levels at ca. 10,500 cal yr BP. These data suggest more and larger fires than before likely as a result of increased *Picea* abundance on the landscape. Fire episodes and BCHAR decreased with the decline of *Picea* at ca. 9000 cal yr BP. Fire activity increased again from 3 to 5 episodes 1000 yr^{-1} at Fairy Lake from ca. 9000 to 8000 cal yr BP in association with an expansion of *Pseudotsuga* and *Pinus albicaulis and/or P. flexilis.* The fact that BCHAR did not increase at this time suggests that area burned remained constant, even though fire episodes were more frequent than before. Krause et al. (2015) suggests that more frequent fires in the NRM may have led to more open landscapes in the early Holocene, which also seems to be the case at Fairy

Lake. The increase in herbaceous plant taxa, such as *Ambrosia*, Amaranthaceae, and Asteraceae, support the interpretation of a more open landscape. Fire activity at Dailey Lake decreased as the landscape became more open in the early Holocene, starting ca. 10,000 cal yr BP (Krause et al., 2015). Fire activity was low at Crevice Lake before ca. 8000 cal yr BP, and then increased from 8000 to 7000 cal yr BP (Whitlock et al., 2012). Blacktail Pond had high fire activity during this period, particularly at ca. 8000 cal yr BP (Krause & Whitlock, 2013). Fire activity at Slough Creek Lake also experienced an increase in fire activity at ca. 8000 cal yr BP (Millspaugh et al., 2004).

Summer insolation reached its maximum between 11,000 and 9000 cal yr BP, bringing warmer-than-present summer temperatures and enhanced monsoonal moisture to the region. Strengthened monsoonal circulation from the Gulf of Mexico and Gulf of California (Whitlock & Bartlein, 1993) or greater winter precipitation (Whitlock et al., 2012) promoted wetter conditions in the summer-wet areas within the northern GYE (Whitlock & Bartlein, 1993). Marl-rich sediments are associated with the precipitation of $CaCO_3$, caused by warmer water temperatures. Fairy Lake also had a spike in carbonate content within this timeframe, suggesting warmer water temperatures or lower lake levels. In the early Holocene, increased fire activity and marl deposition at Blacktail Pond suggest effectively drier summers than before or at present (Huerta et al., 2009). The $\delta^{18}O$ record at Blacktail Pond indicate a sharp increase in temperature and evaporation at this time, providing evidence of higher-than-before summer temperatures (Krause & Whitlock, 2013). The $\delta^{18}O$ record at Crevice Lake implies increased winter precipitation, in agreement with paleoclimate models that suggest a northward shift of winter storm tracks (Bartlein et al., 1998, Whitlock et al., 2012).

Middle Holocene Period (ca. 7100 to 3000 cal yr BP).

An increase in *Pseudotsuga/Larix* pollen in the middle Holocene at Fairy Lake suggests an upslope spread or higher density of *Pseudotsuga* in the Bridger Range with less *Pinus albicaulis and/or P. flexilis* than previously. *Artemisia* percentages decrease from the previous period while those of Total Rosaceae, Asteraceae sub. Asteroideae, Other Amaranthaceae, *Ambrosia*-type and Other Herbs increase, indicating a more open landscape than before. High percentages of *Sarcobatus* pollen indicate higher amounts of *Sarcobatus* than before down valley or in dry settings farther east, supporting a drier environment than before. Pollen increases of *Juniperus*-type and *Shepherdia canadensis* likely come from understory taxa growing within the scattered stands of *Pseudotsuga*. Increased percentages of *Potamogeton* suggest the lake was more productive than before and high values of *Alnus* percentages indicate possibly shallower conditions, as the plant species may have colonized the available riparian area from a receding water body. The lithologic data show rising organic content from previous conditions, aligning with an increase in lake productivity, and the carbonate content increased from previous conditions, in agreement with decreasing, but higher-than-present summer temperatures. Pollen data suggest a shift to *Pseudotsuga* parkland ca. 7000 cal yr BP at Slough Creek Pond (Millspaugh et al., 2004), at ca. 8000 cal yr BP at Crevice Lake (Whitlock et al., 2012), and at ca. 7600 cal yr BP at Blacktail Pond (Huerta et al., 2009). In contrast, the shift occurred quite early at ca. 10,200 cal yr BP at Dailey Lake, likely as a result of Dailey Lake's lower elevation (1598 m elevation) (Krause et al., 2015).

Fire episodes at Fairy Lake were frequent in the middle Holocene, ~ 4-6 episodes 1000 yr^{-1}, but low BCHAR values indicate low levels of biomass burning suggesting fires were small or largely ground fires, supporting the idea of an open landscape. Crevice Lake fire activity decreased between ca. 7000 and 5000 cal yr BP, and then increased between ca. 5000 and 4000 cal yr BP (Whitlock et al., 2012). Blacktail Pond fire activity was lower from ca. 7600 to 4000 cal yr BP than before (Huerta et al., 2009). Slough Creek Lake had high fire activity between ca. 8000 and 6000 cal yr BP, decreased levels from ca. 6000 to 5000 cal yr BP, and a steady increase into the late Holocene (Millspaugh et al., 2004).

Paleoclimate model simulations for the middle Holocene show a change to less precipitation and warmer winters than before in the central U.S. (Bartlein et al., 1998, Shinker et al., 2006). This shift is explained by increasing winter insolation, higher than present but declining summer insolation, and decreasing monsoonal circulation (Whitlock & Bartlein, 1993, Bartlein et al., 1998). Mean July temperatures were higher than before during the middle Holocene for the Pacific Northwest (Fig. 13) (Viau et al., 2006). The decline in precipitation for the region is evident in the transition to *Pseudotsuga* parkland at most sites as well as increased fire activity in the northern GYE. Lake level decreases in the Rocky Mountains during the middle Holocene are also evidence of arid conditions in the region (Shuman et al., 2009).

Late Holocene Period (ca. 3000 to 745 cal yr BP).

After ca. 2500 cal yr BP, the pollen data suggest a decline in *Pseudotsuga* at Fairy Lake and the establishment of mixed-conifer forest composed of *Pinus, Picea,* and *Abies*. The increase of *Populus,* Roseaceae, Poaceae, Asteraceae, *Ambrosia,* and other herbaceous species during this period suggest that an expansion of meadows and aspen groves on south-facing slopes. The pollen increase in *Potamogeton* and Other Aquatics (e.g., *Equisetum, Pediastrum*) indicates that the lake became more productive than before, and decreased percentages of *Alnus* imply more limited riparian areas and possibly rising water levels. The lithologic data show a decrease in organic material, which may be related to the decrease in *Alnus*, or lake levels rising and lake stratification. The carbonate levels in the lake are steadily decreasing with the exception of an increase at ca. 1000 cal yr BP. This could be the result of a warmer period, increased lake pH, or lake stratification. The high amount of *Sarcobatus* pollen in the late Holocene may indicate drier conditions in the valleys. Crevice Lake experienced an expansion of *Pseudotsuga* and *Pinus* and a reduction of *Juniperus* after 3000 cal yr BP (Whitlock et al., 2012). The expansion of *Artemisia* steppe and *Pseudotsuga/Pinus* parkland in the late Holocene at Blacktail Pond is similar to vegetation developed at Slough Creek Lake in the middle Holocene (Millspaugh et al., 2004, Huerta et al., 2009).

Fairy Lake fire frequencies were lower in the late Holocene than before, decreasing from ~6 to 4 episodes 1000 yr^{-1}. In contrast, overall CHAR and BCHAR levels were high, indicating that fires were larger and likely stand replacing, similar to those in the subalpine forests today (Schoennagel et al., 2004). Fire activity at Crevice Lake increased slightly from previous conditions at ca. 3000 cal yr BP, but decreased toward present day (Whitlock et al., 2012). Blacktail Pond fire activity was initially similar to that of the previous period, ~ 5 episodes 1000 yr^{-1}, but fire frequency decreased towards present day (Huerta et al., 2009). Slough Creek Lake experienced increasing and highest fire activity in the late Holocene, reaching ~ 12-17 fire episodes 1000 yr^{-1} (Millspaugh et al., 2004). It has been speculated that the high fire activity at Slough Creek Lake in the late Holocene was a result of increased summer drought (Millspaugh et al., 2004) or increased ignitions from convective storms coupled with a more open landscape with fine fuels promoting fire spread (Huerta et al., 2009).

The late-Holocene vegetation and fire history at Fairy Lake suggests cooler and more humid conditions than before. Paleoclimate model simulations for this time period indicate cooler and effectively drier conditions are a result of declining summer insolation and weakened monsoons (Bartlein et al., 1998). An increase in aridity is evidenced by expansion of *Artemisia* steppe and *Pseudotsuga* and *Pinus contorta* parkland and a decline in *Picea* at both Slough Creek Lake and Blacktail Pond (Huerta et al., 2009). The $\delta^{18}O$ record at Crevice Lake reveals an overall trend of declining winter precipitation, with a few periods of increased winter precipitation (Whitlock et al., 2012). In contrast, Fairy Lake shows wetter conditions than before as evidenced by the expansion of *Abies, Picea*, and *Pinus*. The wetter conditions at Fairy Lake in the last 3000 cal yr may be the result of elevation. An additional explanation might be greater snowpack on the east side of the Bridger Range because of northwestern mountain range alignment that funnel winter storm tracks laden with moisture (Birkland & Mock, 1996)

The Medieval Climate Anomaly (MCA) (1200 – 800 cal yr BP) is not evident in the pollen record at Fairy Lake, but within the NRM, drought is generally registered by an increase in fires. Crevice and Slough Creek lakes show an increase in fire activity (Millspaugh et al., 2004, Whitlock et al., 2012). Drought at this time is also evidenced by post-fire debris flows (Meyer et al., 1995) and reduced beaver activity (Persico & Meyer, 2009) in the northern GYE.

The Fairy Lake cores have several thick red bands of clay (Fig. 5) that were likely deposited in the lake by fluvial activity, including a thick layer that dates to 920 cal yr BP. The sediment comes from outcrops of Amsden Formation on the southwest side of the lake (Bodalski & Michels, 2014, *unpublished data*). The layers were probably deposited during years of rapid snowmelt, when warmer conditions destabilized snowpack and led to rapid run-off, or possibly during periods of frequent heavy summer convective rain.

Humans are known to have been present in and around the Bridger Range. Some of the earliest evidence of humans in the western U.S. comes from a burial site that dates to 12,707 – 12,556 cal yr BP, located 25 km east of Fairy Lake in the Shields Valley (Rasmussen et al., 2014). Archaeological findings, such as various lithics and some stone cairns, in the Bridger Range reveal regular use of the mountains during the period from 13,000 to 300 BP for hunting, gathering and food processing (Table 4)(Byers et al., 2003). (Archaeological dates are discussed in uncalibrated ^{14}C) Stone tools were discovered in the Fairy Lake watershed and a pictograph, hunting camps and possible burials have been found elsewhere in the Bridger Range (M. Pablo, personal communication, 01/2014). The stone tools are associated with Pelican Lake projectile point styles, which date to ca. 3000 – 1500 BP (Darroch, n.d., MacDonald, 2012). Archeologists suggest that Fairy Lake and the Bridger Range in general were used in a transient and seasonal manner (Byers et al., 2003, Fisher et al., 2016). The archeological record provides no information on whether or how ancient people used fire, aside from campsite activities, and there is little evidence that people significantly altered the vegetation at Fairy Lake. If there was an anomaly in the fire record of Fairy Lake that is not seen in other regional records, then it might be possible to attribute such anomalies as anthropogenic, however, as of now, no anomalies have been detected.

Humans inhabiting the Pacific Northwest have used fires to maintain prairies, cultivate berry crops, and communication (Boyd, 1999; French, 1999; Barrett & Arno, 1999). The burial site in the Shields Valley shows that humans have been present in the region since the late glacial. In addition, three artifacts (dacite points) found within the Bridger Range have been assigned to the Paleoindian period (ca. 12,000 – 8000 BP) showing that humans have made use of the area for millennia (Table 4)(Fisher et al., 2016). Hence, it could be speculated that humans would have employed fire to promote food resources (e.g., *Vaccinium*) but the Fairy Lake record provides little direct evidence of human influence. At ca. 12,500 cal yr BP, CHAR and BCHAR increase for a short time period, ca. 500 years. Previously in this text, this increase was attributed to the rising levels of fuel during the late-glacial period from increased *Picea*. However, an alternative explanation is that humans caused this increase in fire activity during the late-glacial period by increasing the amount of ignitions as fuels became more available. Similarly, an increase in CHAR and BCHAR from 3000 to 745 cal yr BP aligns evidence of human presence at Fairy Lake during the Pelican Lake archeological period (ca. 3000 – 2500 BP).

The forest was more closed at this time, and humans may have acted as an ignition source in addition to lightning. In addition, high levels of CHAR and BCHAR at Fairy Lake during are associated with two increases in effective moisture based on

Table 4. Select archaeological artifacts found in the vicinity of Fairy Lake.

Archaeological period /Age[1]	Artifact	Region	Source
Early Paleoindian / ~12,631 cal yr BP	Human burial	Shields Valley	Rasmussen et al., 2014
Paleoindian / 12,000 – 8000 BP	3 dacite projectile points	Bridger Range	Fisher et al., 2016
Early Archaic / 8000 – 5000 BP	1 dacite projectile point	Bridger Range	Fisher et al., 2016
Middle Archaic / 5000 – 3000 BP	3 dacite, and 2 obsidian projectile points	Bridger Range	Fisher et al., 2016
Late Archaic / 3000 – 1500 BP	11 dacite, and 8 obsidian projectile points	Bridger Range	Fisher et al., 2016
Late Precontact 1500 – 300 BP	3 dacite, and 3 obsidian projectile points	Bridger Range	Fisher et al., 2016

1: Calibrated ^{14}C dates listed as “cal yr BP” and uncalibrated ^{14}C dates listed as “BP”.

changes in lake-level at Lake of the Woods located in the Wind River Mountains, ~250 km from Fairy Lake; one at ca. 2600 cal yr BP and one at ca. 1900 cal yr BP (Kelly et al., 2013). The inferred periods of increased effective moisture at Lake of the Woods also coincide with an increase in human population size in the Bighorn Basin, located ~275 km from Fairy Lake, between the GYE and the Bighorn Mountains (Kelly et al., 2013). As described by Kelly et al. (2013), it is plausible that the growth of human populations associated with increases in effective moisture thereby led to increases in CHAR at Fairy Lake. Increased populations need more resources, and have wider geographic footprints, and increased fire activity from human ignitions in the Shields Valley may have registered in the Fairy Lake record. The Fairy Lake records increases of CHAR and BCHAR during these periods of human population size in the region but it is not possible to directly attribute these changes to deliberate human-set fires.

Regional Comparison of Vegetation History

The number of pollen records in the NRM enables a comparison of the Fairy Lake record with sites across a broader region. Hoodoo, Baker, Pintlar, Floating Island, Beaver, and Sherd lakes were examined along with the records discussed previously in the northern GYE. For more information on these sites, refer to Table 3.

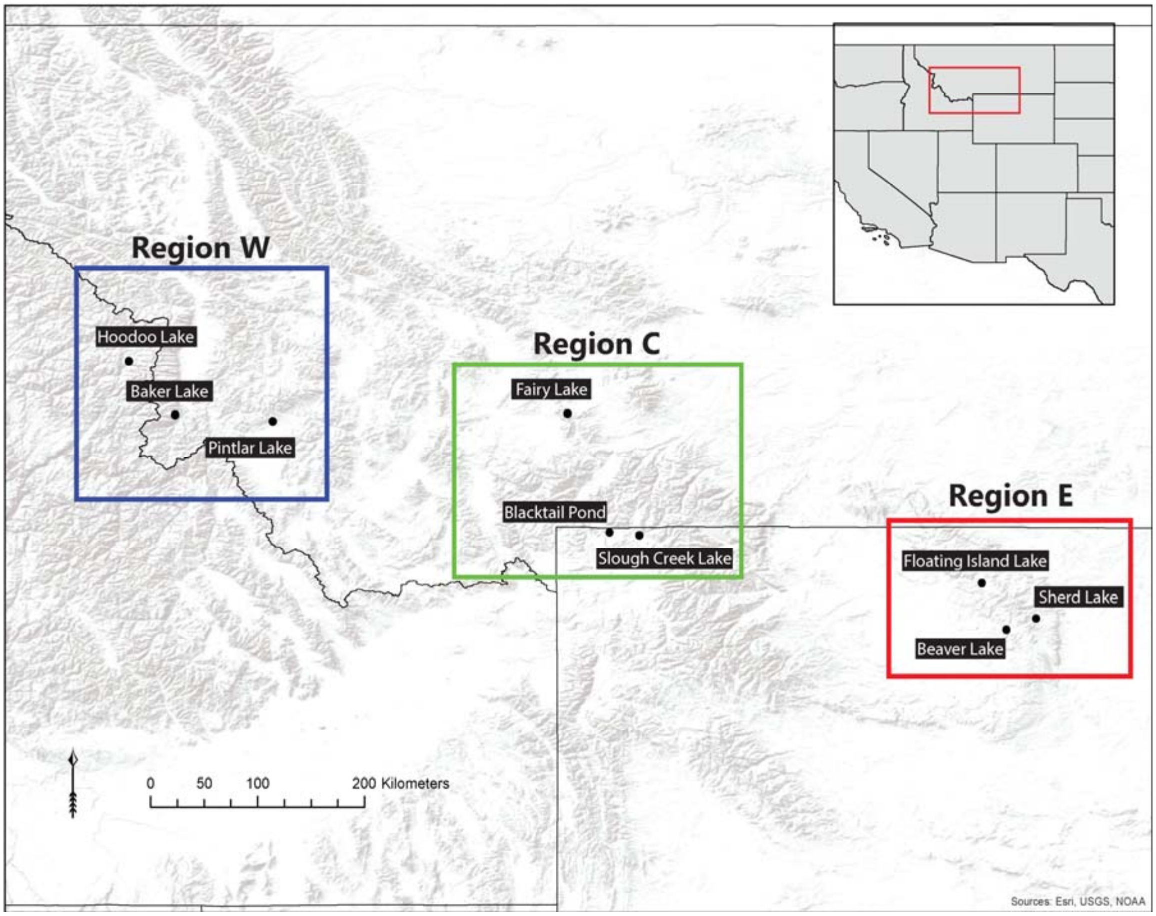

Fig. 9. Sites selected in the western NRM (Region W), central NRM (Region C), and eastern NRM (Region E). See Table 3 for site information.

The NRM was divided into three regions: the western region, Region W, includes Baker Lake, Hoodoo Lake, and Pintlar Lake in the Bitterroot/Selway region. The central region, Region C, is represented by three records within the northern GYE: Fairy Lake, Blacktail Pond, and Slough Creek Lake. The eastern region, Region E, includes Floating Island Lake, Beaver Lake, and Sherd Lake in the Bighorn Mountains of north-central Wyoming, (Fig. 9). Climate data from several different records spanning from 1894 to 2016 (Western Regional Climate Center, 2016) were used to determine if a region was more summer-wet or summer-dry, based on the total average amount of precipitation received in June, July and August, divided by the amount of precipitation received in December, January, and February. Values > 1 were classified as summer-wet, and values $\leq$ 1 were considered summer-dry. Pollen data were obtained from the Neotoma Database (neotomadb.org) and the North Central Climate Science Center Paleoenvironmental Database. (http://www.nccscpaleoenvironmentaldatabase.com).

Two of the sites in Region W are summer-dry (Hoodoo = .41, Baker = .96). Pintlar Lake is summer-wet (2.8). Conversely, Regions C & E are located in the summer-wet regions, receiving higher levels of moisture in summer from convective storm systems (Fairy = 1.3, Crevice = 2.8, Blacktail = 1.7, Slough Creek = 1.5, Floating Island = 1.8, Beaver = 2.1, Sherd =3.4).

Relative pollen abundances of Poaceae, Amaranthaceae (including *Sarcobatus*) and *Artemisia* were plotted through time to see whether differences in summer-wet and summer-dry conditions were maintained through the late-glacial to the late Holocene (Fig. 10). High percentages of *Artemisia* pollen indicate relatively wet conditions and high values of Amaranthaceae indicate the driest conditions. The ratio of *Artemisia* to Amaranthaceae pollen has been used in other studies to detect changes in moisture, with increases in *Artemisia* indicating more available moisture (Wigand, 1987, Mensing et al., 2004, Brunelle et al., in review). High pollen percentages of Poaceae relative to *Artemisia* have also been attributed to decreases in effective moisture or decreases in winter precipitation in the GYE (e.g., Huerta et al., 2009).

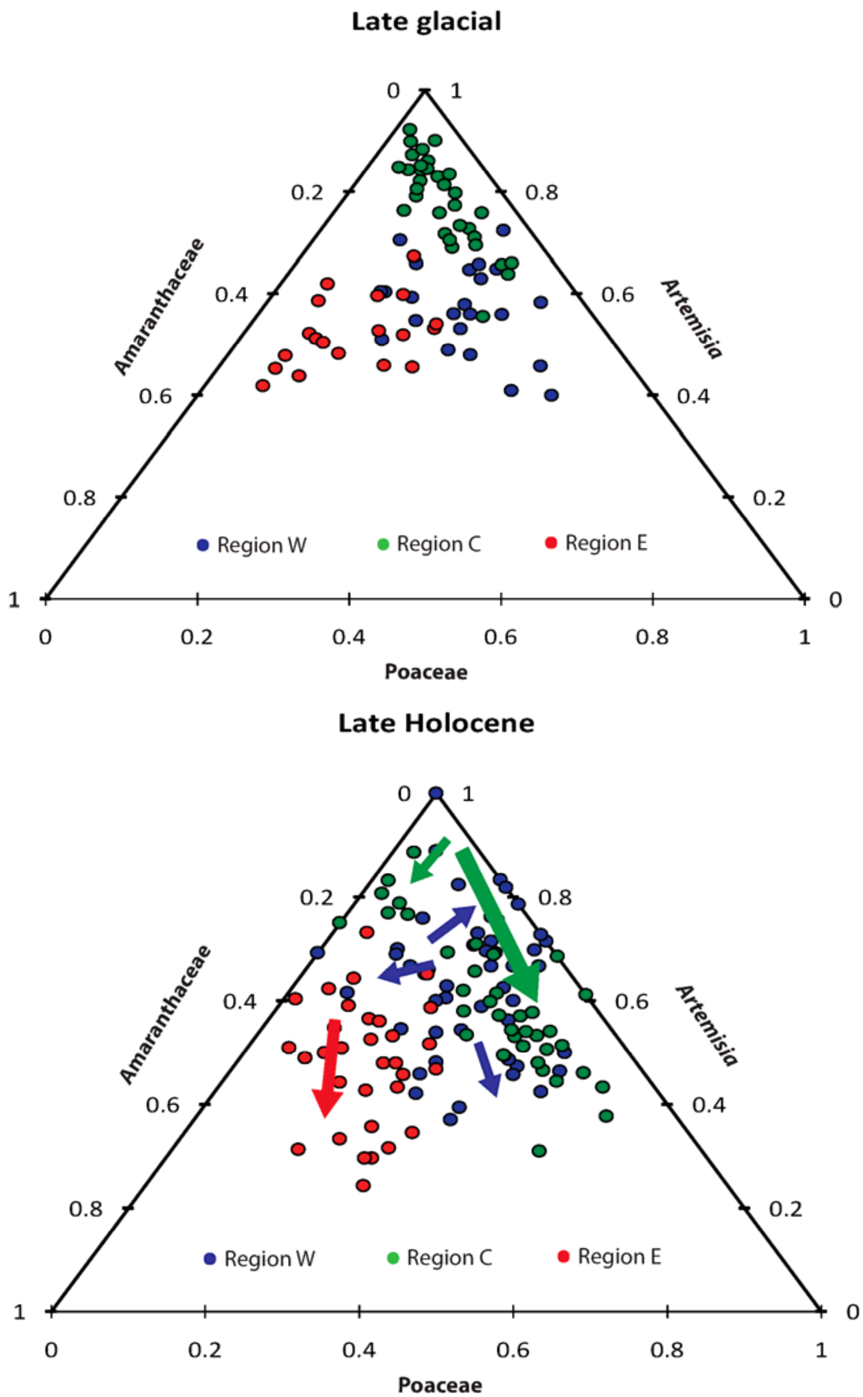

Fig. 10. Three pollen taxa from the different regions in two different time periods. The top diagram is the late glacial period (~15,500 – 10,500 cal yr BP) the bottom diagram is the late Holocene (3000 – 0 cal yr BP). The closer the dot is to a side of a triangle, the more of that taxa is present. Colored arrows on the bottom graph show changes in composition.

The three regions show clear differences. In the late-glacial, Region W (summer-dry) had more *Artemisia* pollen than Poaceae or Amaranthaceae pollen, Region E (summer-wet) had more Amaranthaceae, and Region C (summer-wet) had equal amounts of *Artemisia* and Amaranthaceae pollen and less Poaceae pollen (Fig. 10). In the late Holocene, the three regions are more variable, but maintain some interregional differences. Region W is an intermediate between Region E and C based on what specific evidence. Region E seems to have a more restricted distribution than the other two. Region E seems to be more similar to the other sites in the late-glacial period, showing high values of what that indicate wet conditions. Region E shows a shift toward drier conditions in the late Holocene, based on increased Poaceae and Amaranthaceae. Region C registers more *Artemisia* and less Poaceae pollen in the late-glacial period, indicating wet conditions. The differences among the three regions seem to be more pronounced and more sharply defined in the late-glacial period, which implies that that period was most different from present conditions in the late Holocene.

The ratio of arboreal pollen to non-arboreal pollen (AP/NAP) identifies changes in forest cover related to variations in temperature, effective moisture and disturbance (e.g., Herzschuh, 2007, Li et al., 2010, Whitlock et al., 2012, Mumma et al., 2012, Krause & Whitlock, 2013, Krause et al., 2015). In general, an increase in AP over NAP pollen indicates more forest cover and moister and possibly warmer conditions (Krause et al. 2015), although lower AP/NAP values may also be the result of drier and warmer conditions, and increases in effective moisture can also occur during cooler periods.

The AP/NAP ratio for each site in each region was calculated, then normalized ((Total AP – Total NAP) / (Total AP + Total NAP)) and plotted through time (Fig. 11). The data reveal a few interesting trends. First, during the late-glacial period, ca. 15,500 – 10,000 cal yr BP, almost all of the records have less arboreal taxa than at present, with the exception of high-elevation Baker Lake, which shows AP/NAP values similar to present day. As temperatures increased in the late-glacial and into the early Holocene (ca. 11,500 – 10,000 cal yr BP), all sites show increasing forest abundance. Second, by ca. 9500 cal yr BP, all sites feature an additional increase in AP/NAP ratios, marking the onset of greatest forest cover. This second increase occurred within the early Holocene at most sites, which was a time of higher-than-present temperatures and longer growing seasons in the NRM. After ca. 6000 cal yr BP, all sites show more forest cover than before (e.g., high AP/NAP), with the exception of Blacktail Pond. Modern AP/NAP levels were established at ca. 3000 cal yr BP at most sites. The sites in Region C show the largest fluctuations in the AP/NAP ratio through time. These fluctuations could be a result of their position at the transition between the summer-wet and summer-dry precipitation regimes, in which case the variability results from shifts along the west-to-east moisture gradient, with the center region (Region C) showing the highest moisture fluctuations through time, while the east region (Region E) remains relatively dry, and the west region (Region W) remains relatively wet. At times, individual sites within Region C are more similar to those in Region E (drier), and at other times, they are more similar to Region W (moister).

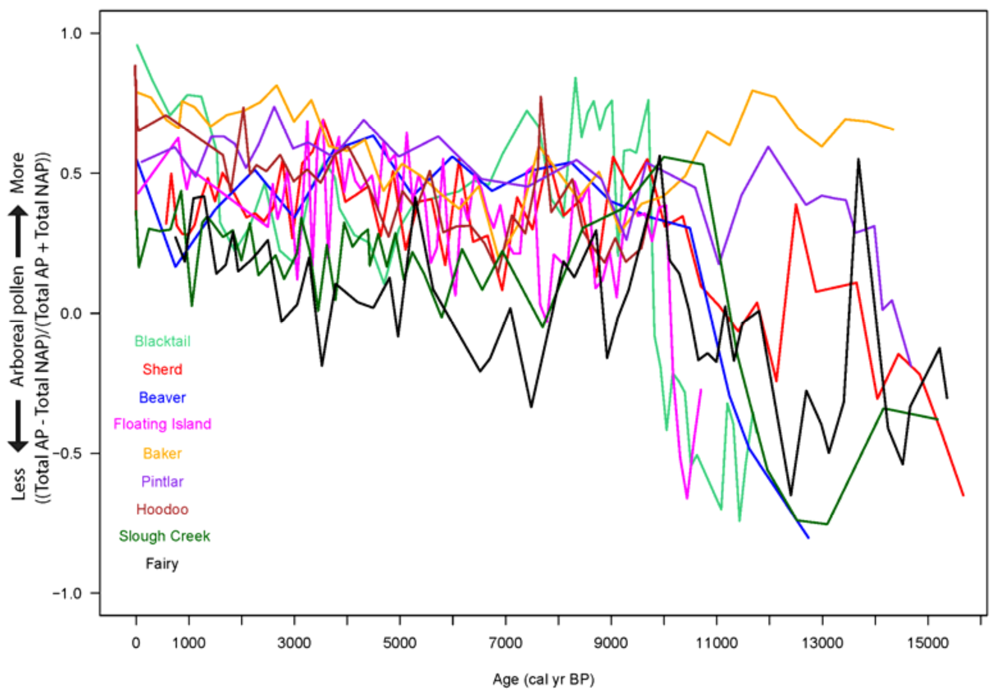

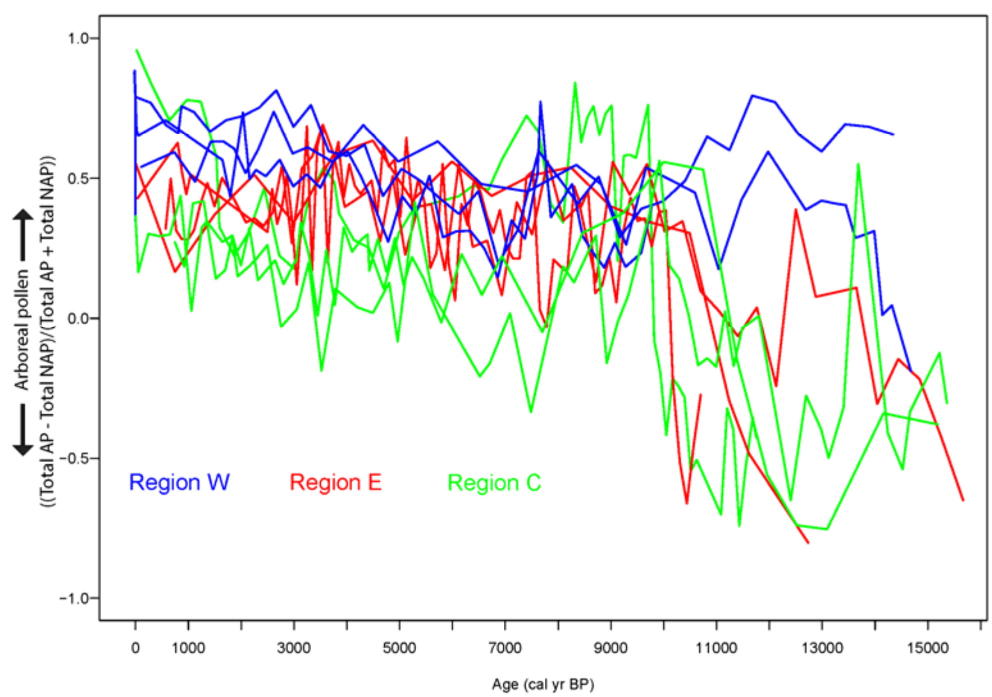

Fig. 11. Ratio of arboreal to nonarboreal pollen (AP/NAP) for selected sites. The top graph are the individual sites, and the bottom graph are the sites

An alternative explanation for the variability in Region C is that the elevational differences between sites in Region C account for variable levels of AP/NAP. Fairy Lake is the highest of the Region C sites at 2306 m elev, and then Blacktail Pond at 2012 m, followed by Slough Creek Pond, located at the lowest elevation 1884 m.

However, the elevational differences between sites in Region W are as great as Region C, with Baker Lake at a similar elevation as Fairy Lake, followed by Pintlar Lake at 1921 m, and Hoodoo Lake at 1700 m. The sites within Region W did not experience as much variation as in Region C, suggesting that elevational differences in the west may have been less of a factor than in the northern GYE for the expansion or contraction of forests.

Separating sites by their summer-wet, summer-dry classification reveals some interesting patterns. The sites in the summer-wet and summer-dry regimes are distinguishable from each other through most of their history (Fig. 12). The summer-dry sites overall registered more arboreal pollen through the record. This observation supports ecological studies that suggest winter precipitation is more important for the growth of arboreal taxa and forest greenness than summer moisture (Hu et al., 2009, Trujillo et al., 2012). In contrast, the summer-wet sites show more variability in tree abundance, and more or less show similar trends in tree abundance through the record. This temporal pattern supports ecological studies that point the importance of summer convective storms for grassland development (Thompson et al., 1996).

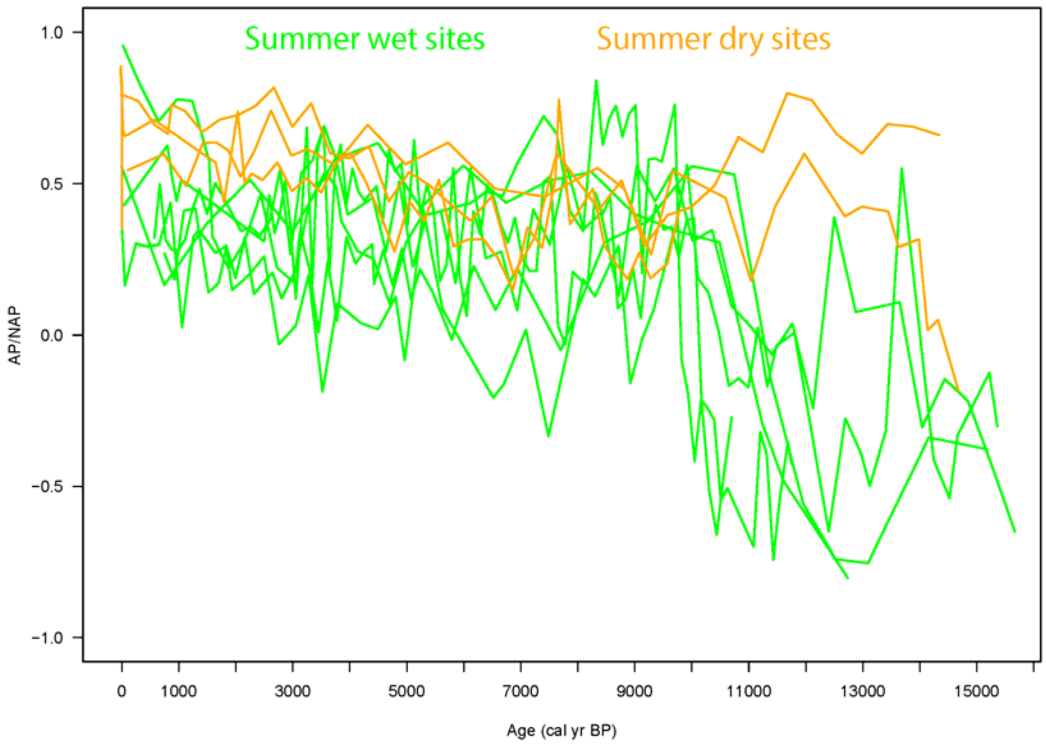

Fig. 12. Ratio of arboreal to nonarboreal (AP/NAP) at summer-wet and summer-dry sites over the last 15,500 cal yr BP

The mean AP/NAP ratio in each region was calculated by interpolating the data from that region and compared with an independent 14,000-year-long reconstruction of mean July temperature (Viau et al., 2006) to help understand regional changes in AP/NAP. The reconstruction is based on 84 different temperature-derived pollen studies from the Pacific Northwest., (Fig. 13). The comparison suggests that, as temperatures increased from the late-glacial period to present day, so did the abundance of forest cover at all sites. What is interesting, is the smaller, short-term changes. For example, at ca. 6900 cal yr BP, Regions W & E show decreases in arboreal taxa in association with a period of lowered temperatures, while Region C registers an increase in arboreal taxa (Fig. 13). This may be the result of Region C being between the other two Regions, and perhaps had moderate amounts of both kinds of annual precipitation, at this point in time.

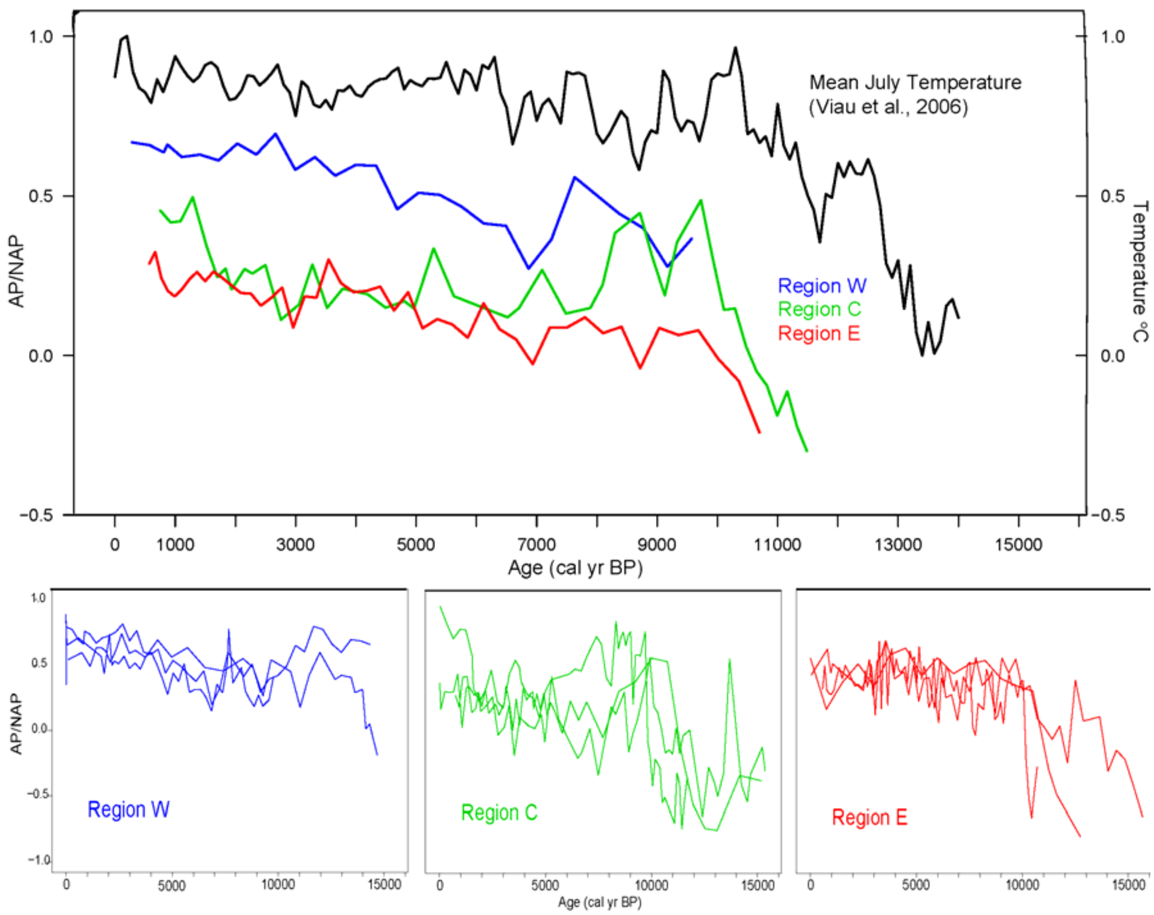

Fig. 13. Top graph shows the mean AP/NAP pollen ratio for each region, and mean July temperature (Viau et al., 2006). Bottom three graphs show AP/NAP data for three sites from each of the different regions.

NRM Fire Records

Fire is governed by regional climate patterns, vegetation composition and structure, and local site characteristics (slope, elevation, aspect), and it is often difficult to compare charcoal abundance or local fire-episode frequency data from sites in different regions without some kind of standardization. Fire-history studies often standardize charcoal data by calculating the z-score of CHAR records for more meaningful comparisons (e.g., Carter et al., 2013, Power et al., 2011). A z-score calculation was employed with the CHAR data from Burnt Knob Lake, Baker Lake, Fairy Lake, Cygnet Lake, Blacktail Pond, Crevice Lake, and Slough Creek Lake. Charcoal datasets were accessed from the NOAA global charcoal database (paleofire.org) as well as the North Central Climate Science Data Center (http://www.nccscpaleoenvironmentaldatabase.com).

The three-step method used by Blarquez et al. (2014) was used to transform the data (minimax, box-cox, z-score calculation). R was used for the computation of this transformation. The base period for all calculations was the last 3000 years, as this is the timespan when pollen data indicate the establishment of modern forests in the NRM and the charcoal records are based on nearly complete CHAR data. In order to see how the Fairy Lake charcoal record compared with the other records, all charcoal data were plotted together, using a black line for all sites but Fairy Lake, which was plotted in a red

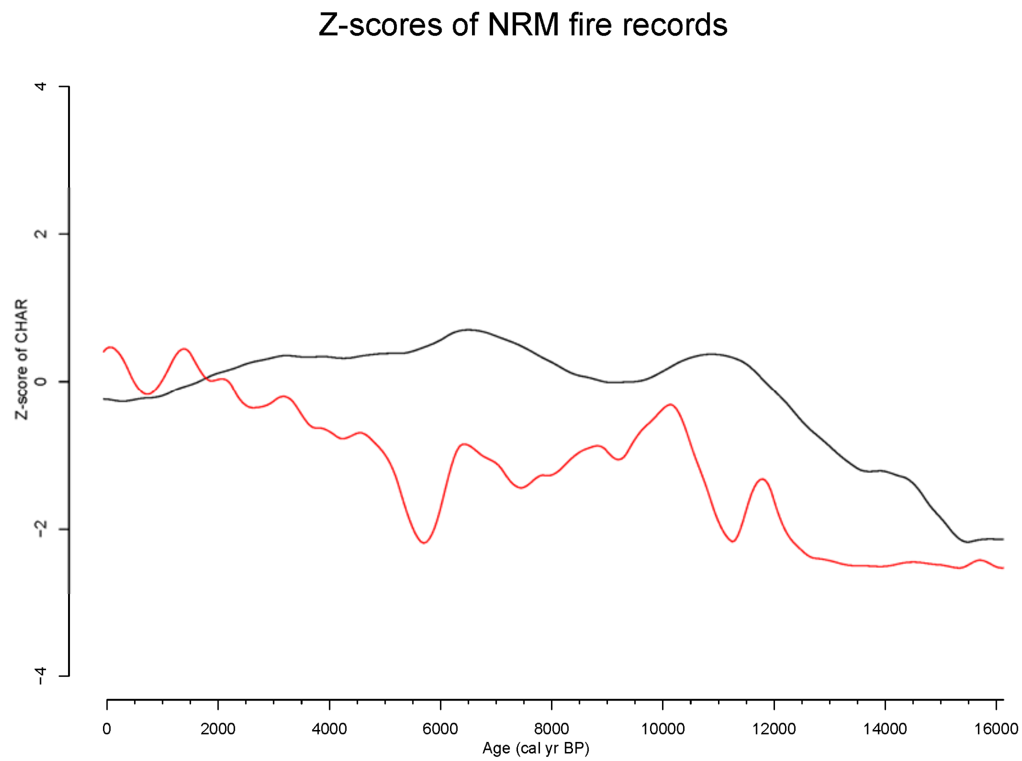

Fig. 14. CHAR z-scores from NRM records, Fairy Lake in red, composite scores from all other sites in black. Zero represents the relative mean of each line. The base period for comparison of all records is the last 3000 years in each record.

line (Fig. 14). The Fairy Lake data were similar to the other sites in the NRM in showing positive charcoal anomalies in the late-glacial period, ca. 12,000 – 10,500 cal yr BP, and in the late Holocene period, ca. 3000 – 0 cal yr BP. Unlike other sites, the Fairy Lake record did not record high positive anomalies in the early and middle Holocene (ca. 10,000 – 3000 cal yr BP). The datasets were grouped by their contemporary summer-wet/summer-dry classifications as was done with the pollen comparisons above (Fig. 15). The charcoal records of summer-dry sites show large negative anomalies from the mean

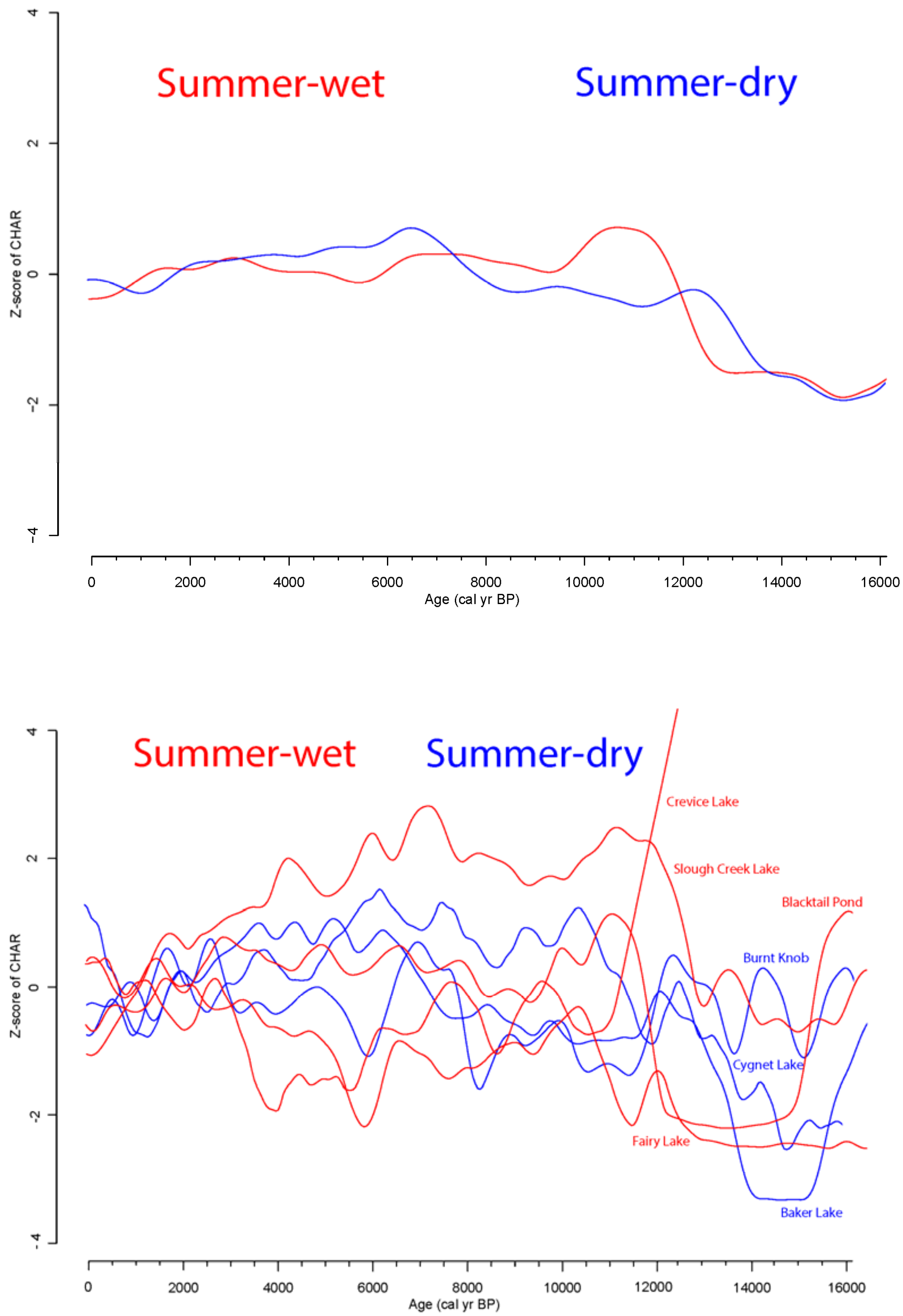

Fig. 15. Comparison of CHAR z-scores by their summer-wet/summer-dry classification.

between ca. 12,000 and 7500 cal yr BP and larger positive anomalies from the mean starting at ca. 7500 cal yr BP that persist until ca. 3000 cal yr BP.

The means from the regions, graphed together (Fig. 15, top graph) show an interesting pattern, where one region tends to have higher than average fire activity, the other does not, and vice versa. Furthermore, in the late-glacial and early Holocene periods, ca. 12,000 – 7100 cal yr BP, the summer-wet areas have higher fire activity than the summer-dry. The opposite is true for the middle Holocene, ca. 7100 – 300 cal yr BP.

The late-glacial and early Holocene periods are times associated with increased wetness in the summer-wet areas, and this time period also includes some of the highest AP/NAP ratios for the summer-wet region (Fig. 11, 12), leading to the conclusion that increased wetness, led to increased forest cover, which created fuel conditions that led to increased fire activity. In the summer-dry areas, the middle Holocene (ca. 7100 – 300 cal yr BP) was the time of the most fire activity. As discussed above, this is a time associated with increased aridity in the NRM. The forest cover in the summer-dry sites is higher than in most summer-wet sites throughout the record, and so an increase in aridity seems to have led to more fires in the summer-dry areas. Aridity seems to be the factor that leads to more fires in the western region in the past, whereas increased precipitation along with increased temperatures led to more fire activity in the center and eastern regions.

Among summer-wet sites, Slough Creek Lake differs from the other records. Overall, it has much higher departures from the mean, especially during the late-glacial period (ca. 15,000 –10,500 cal yr BP) and middle Holocene (ca. 7100 — 3000 cal yr BP). This may be a result of its relatively low elevation (1884 m). Crevice Lake is also at a low-elevation site (1713 m), but it is located in a canyon and may have been more protected from fires. The combination of low elevation and its openness may explain the higher fire activity at Slough Creek Lake. In summer-wet regions, conditions became progressively moister and warmer at the end of the late-glacial period, and a strengthening of the summer monsoonal circulation may have increased convective storms and lightning-started fires (Whitlock & Knox, 2002). In the late Holocene, summer-wet sites generally became drier than present and experienced periods of extended drought (e.g., MCA). This was also a time when most sites were developing more closed forests, leading to more fuel availability during drier periods, and positive fire anomalies in the late Holocene.

In summer-dry regions, the late-glacial period was a time of increased winter precipitation, likely supporting the growth of forest taxa, but conditions were cooler and wetter than at present and this likely suppressed fire activity. A period of aridity in the summer-dry regions occurred in the middle Holocene (ca. 7100 – 3000 cal yr BP) (Whitlock & Bartlein, 1993), and fire activity was high during this period (Fig. 15). Sites located in the summer-dry western region also register higher-than present fire activity at this time (Whitlock et al., 2008). Perhaps these regional differences are related to fuel difference as implied in the AP/NAP relationships between the regions discussed earlier. The summer-dry sites had more woody fuels during the 9000 - 3000 cal yr BP period than most of the summer-wet sites (Fig. 11, 12), and this may have heightened fire activity in the early and middle Holocene.

CONCLUSIONS

The Fairy Lake record provides the first information on the postglacial vegetation and fire history of the Bridger Range. The site initially was covered by tundra-steppe following glaciation, ca. 15,500 cal yr BP. *Alnus, Betula, Salix* and *Juniperus* were the first shrubs to colonize following deglaciation. *Picea* parkland developed ca. 11,300 and persisted until ca. 9000 cal yr BP when it was replaced by an open forest of *Pinus albicaulis* and/or *P. flexilis* with some *Picea* and *Abies. Pseudotsuga* expanded at lower elevations from ca. 9000 to 3000 cal yr BP. Overall, *Pinus, Picea* and *Abies* decreased, and *Pseudotsuga* increased at ca. 7100 cal yr BP. The abundance of *Sarcobatus* pollen during the middle Holocene along with significant percentages of *Pseudotsuga/Larix* pollen provide evidence of the expansion of parkland at lower elevations. The vegetation in the Fairy Lake watershed was likely more open during the early and middle Holocene than it is today. In the last 3000 cal years, a closed mixed conifer forest of *Picea, Abies, and Pinus* was established at the lake. The lake also experienced likely transitions from a shallower, unproductive system in the early Holocene, a shallow and more productive system in the middle Holocene and finally to a deeper, possibly more stratified system in the late Holocene.

The Fairy Lake vegetation record is similar to other northern GYE records, except that its pollen record registered the arrival and expansion of *Picea* about 1325 years later than at other sites. Similarly, the presence of *Pseudotsuga* occurred ~1600 years earlier than at other northern GYE sites. These differences may be the result of the high-elevation location of Fairy Lake, which may have suppressed temperatures and reduced moisture loss, or led to an increase in overall snowpack. The Fairy Lake fire history recorded an initial period of low fire activity, followed by a slight increase in fires associated with the development of *Picea* parkland. The middle Holocene registered an increase in fire-episode frequency, but an overall decrease in biomass burned. The more open landscape and drier-than-present climate supported frequent but small fires. In the late Holocene, the establishment of a mixed conifer forest at Fairy Lake was associated with infrequent high-severity fires. It was discussed that humans may have had an impact on the fire record of the Fairy Lake area, but it they did, it is ultimately not visible at this time, within the results of this study.

The comparison of Fairy Lake with other sites across an east-to-west transect in the NRM shows that Fairy Lake and other sites in northern GYE had vegetation histories that were intermediate between those in the Selway/Bitterroot and western region and those in the Bighorn Mountains to the east. This gradient is evidenced by differences in forest cover (AP/NAP) that reflect moisture differences with high levels in the west (relatively higher AP) to low levels in the east (relatively lower AP). The northern GYE sites display a greater degree of variation than the other two regions, suggesting that the northern GYE sites vacillated between periods when they were more similar to the western sites and periods when they were more similar to the eastern sites.

Comparing the fire history at Fairy Lake with other NRM sites shows that Fairy Lake is a hybrid between the summer-wet and summer-dry fire records, meaning Fairy

Lake exhibits responses that represent both summer-wet and summer-dry precipitation regimes. The site experienced increased fuel biomass (BCHAR) in the late-glacial period and low levels in the early and middle Holocene. In the late Holocene, Fairy Lake charcoal data again show positive anomalies suggesting a rise in fire activity. The high values in the late-glacial period may be attributed to progressively moister and warmer conditions than before, rising levels biomass and increased ignitions. The middle Holocene decrease in CHAR may been related to a decrease in monsoonal activity, which led to overall lower ignitions and less biomass. The late-Holocene increase in CHAR was likely a result of cooler and, in some places, moister conditions than before, allowing modern mixed-conifer forests to establish. This fire history at Fairy Lake is different from other summer-dry sites, which experienced the highest fire activity in the middle Holocene, most likely as a result greater aridity than before and high forest cover.

Human presence in the region since ca. 13,000 cal yr BP is evident from multiple archaeological records and suggests the possibility for a human influence on fire activity. The vegetation record does not show obvious signs of human activity, but elevated levels of CHAR in the last 3000 years may be related to deliberate burning by humans.

There is value in uncovering new data. Before this research, the vegetation and fire history of the Bridger Range was unknown. This research can now be added to a larger framework of data, allowing a clearer picture of what the post-glacial history of the NRM and GYE to be drawn. Moving forward with a sense of the past provides a sense of ease, and the more we know about the past, the better we can understand future changes. The story of the Bridger Range, will contribute to the mosaic of context of the world in which we live.

REFERENCES CITED

Alley, R. B., 2000. The Two-Mile Time Machine, Princeton University Press, Princeton, NJ.

Arno, S.F., (1979), Forest Regions of Montana, USDA Forest Service Research Paper, INT-218.

Arno, S.F., (1980), Forest Fire History in the Northern Rockies, *Journal of Forestry, 78*(8), pp.460-465.

Bartlein, P.J., K.H. Anderson, P.M. Anderson, M.E. Edwards, C.J. Mock, R.S. Thompson, R.S., Webb, T. Webb III, and C. Whitlock (1998), Paleoclimate simulations for North America over the past 21,000 years: features of the simulated climate and comparisons with paleoenvironmental data, *Quaternary Science Reviews, 17*, 549-585.

Barrett, S. and Arno, S. 1999. Indian Fires in the Northern Rockies. In: Boyd, R. (Ed.), Indians, Fire and the Land in the Pacific Northwest. Oregon State University Press, Corvallis.

Bennett, K.D., Willis, K.J., 2001. Pollen. In: Smol, J.P., Birks, H.J.B., Last, W.M. (Eds.), Tracking Environmental Change Using Lake Sediments. Terrestrial, Algal, and Siliceous Indicators, 3. Kluwer Academic Publishers, Dordrecht. pp. 5 – 32.

Birkeland, K.W., & C.J. Mock, (1996), Atmospheric Circulation Patterns Associated with Heavy Snowfall Events, Bridger Bowl, Montana, U.S.A. *Mountain Research and Development, 16*(3), 281-286.

Blaauw, M. (2010), Methods and code for 'classical' age-modelling of radiocarbon sequences, *Quaternary Geochronology, 5,* pp.512-518.

Blarquez, O., Vannière, B. Marlon, J.R., Daniau, A., Power, M.J., Brewer, S., and Bartlein, P. J. (2014), Paleofire: An R package to analyze sedimentary charcoal records from the Global Charcoal Database to reconstruct past biomass burning, *72*, pp. 255-261.

Bodalski, P. and Michels, R. (2014). X-ray diffraction and scanning electron microscope chemical analysis of Fairy Lake sediment core. Montana State University Dept. of Earth Sciences Mineralogy course (GEO 302) project. *Unpublished*. Bodalp17@gmail.com.

Boyd, R., 1999. Strategies of Indian Burning in the Williamette Valley. In: Boyd, R. (Ed.), Indians, Fire and the Land in the Pacific Northwest. Oregon State University Press, Corvallis.

Brunelle, A., W. Eckerle, K. Petersen, M. Power, and J. Spencer, (2016), A high-resoluton Holocene paleoenvironmental history of Lake Bonneville/Great Salt Lake, GSA Special Paper *in review*, M. Rosen, and S. Starratt (Eds).

Brunelle, A., and C. Whitlock, (2003), Postglacial fire, vegetation, and climate history in the Clearwater Range, Northern Idaho, USA, *Quaternary Research, 60*, pp.307-318.

Brunelle, A., C. Whitlock, P. Bartlein, and K. Kipfmueller, (2005), Holocene fire and vegetation along environmental gradients in the Northern Rocky Mountains, *Quaternary Science Reviews, 24*, pp.2281-2300.

Brunelle, A., W. Eckerle, K. Petersen, M. Power, and J. Spencer, (2016), A high-resolution Holocene paleoenvironmental history of lake Bonneville/Great Salt Lake, *in review.*

Burkhart, M.R., (1976), Pollen biostratigraphy and late Quaternary vegetation history of the Bighorn Mountains, Wyoming, *Ph.D thesis,* University of Iowa Graduate College, Department of Geology.

Byers, D.A., Allen, W., and Fisher Jr., J.W., 2003. Investigations in the Bridger Mountain Range, Montana: *A Backyard Archaeology Project.* In: Kornfeld, M., and Osborn, A.J. (Eds.), Islands on the Plains: Ecological, Social, and Ritual Use of Landscapes. The University of Utah Press, Salt Lake City. pp.142-166.

Carter, V.A., A. Brunelle, T.A. Minckley, P.E. Dennison, M.J. Power, (2013), Regionalization of fire regimes in the Central Rocky Mountains, USA, *Quaternary Research, 80*, pp.406-416.

Daly, C., M. Halbleib, Smith, W. P. Gibson, M. K. Doggett, G. H. Taylor, J. Curtis, and P. P. Pasteris (2008), Physiographically sensitive mapping of climatological temperature and precipitation across the conterminous United States, *Int. J. Climatol.*, *28*(15), 2031–2064, doi:10.1002/joc.1688.

Darroch, J., (n.d.), Fairy Lake “occupation site” Archaeological Survey. Forest Service Survey Report # 01110600129.

Davis, M. B., Brubaker, L. B., and Webb, T. 1973. Calibration of absolute pollen influx. In: Birks, H.J.B. and West, R.G. (Eds.) *Quaternary Plant Ecology: 14th Symposium of the British Ecological Society*, Blackwell, London, pp. 9-25.

Debinski, D.M., K. Kindscher, and M.E. Jakubauskas, (1999), A remote sensing and GIS-based model of habitats and biodiversity in the Greater Yellowstone Ecosystem, *International Journal of Remote Sensing*, *20*(17), 3281-3291.

Dean Jr., W. (1974), Determination of carbonate and organic matter in calcareous sediments and sedimentary rocks by loss on ignition: comparison with other methods, *Journal of Sedimentary Petrology, 44*(1), 242-248.

Despain, D., 1990. *Yellowstone Vegetation.* Robert Rinehart, Inc. Publishers.

Dorn, R.D., 1984. *Vascular Plants of Montana*. Mountain West Publishing, Cheyenne, Wyoming.

Egan, J., R. Staff, and J. Blackford, (2015), A revised age estimate of the Holocene Plinian eruption of Mount Mazama, Oregon using Bayesian statistical modeling, pp.1-14.

Fall, P. L., (1994), Modern Pollen Spectra and Vegetation in the Wind River Range, Wyoming, U.S.A., *Arctic and Alpine Research, 26*(4), pp. 383-392.

Fall, P. L., P.T. Davis, and G.A. Zielinski, (1995), Late Quaternary Vegetation and Climate of the
Wind River Range, Wyoming, *Quaternary Research, 43*, 393-404.

French, D. 1999. Aboriginal Control of Huckleberry Yield in the Northwest. In: Boyd, R. (Ed.), Indians, Fire and the Land in the Pacific Northwest. Oregon State University Press, Corvallis.

Fischer, W.C., and B.D. Clayton, (1983), Fire Ecology of Montana Forest Habitat Types East of the Continental Divide, USDA Forest Service General Technical Report INT-141, May 1983.

Fisher Jr., J.W., M.J. Dudley, and R. Donahoe (2016), Geochemical Analysis of thirty-four projectile points from the Bridger Mountains, Montana. Unpublished report submitted to Heritage Program Lead, Custer Gallatin National Forest, U.S. Forest Service.

Gedye, S.J., R.T. Jones, W. Tinner, B. Ammann, and F. Oldfield, (2000), The use of mineral magnetism in the reconstruction of fire history: a case study from Lago di Origlio, Swiss Alps, *Palaeogeography, Palaeoclimatology, Palaeoecology, 164,* 101-110.

Gosse, J.C., E.B. Evenson, J. Klein, B. Lawn, and R. Middleton, (1995), Precise cosmogenic ^{10}Be measurements in western North America: Support for a global Younger Dryas cooling event, *Geology, 23*(10), pp.877-880.

Grimm, E.C., 1988. Data analysis and display. In: *Vegetation history.* Springer Netherlands. pp.43-76.

Gugger, P.F., and S. Sugita, (2010), Glacial populations and postglacial migration of Douglas-fir based on pollen and macrofossil evidence, *Quaternary Science Reviews, 29*, pp.2052-2070.

Herzschuh, U., (2007), Reliability of pollen ratios for environmental reconstructions on the Tibetan Plateau, *Journal of Biogeography, 34*, pp.1265-1273.

Higuera, P., L. B. Brubaker, P. M. Anderson, F. S. Hu, and T. A. Brown (2009), Vegetation Mediated the Impacts of Postglacial Climate Change on Fire Regimes in the South-Central Brooks Range, Alaska, *Ecological Monographs, 79*(2), pp.201-219.

Higuera, P.E., C. Whitlock, and J.A. Gage, (2010), Linking tree-ring and sediment-charcoal records to reconstruct fire occurrence and area burned in subalpine forests of Yellowstone National Park, USA, *The Holocene, 2*(21), pp.327-341.

Huerta, M.A., C. Whitlock, and J. Yale, (2009), Holocene vegetation-fire-climate linkages in northern Yellowstone National Park, USA, *Palaeogeography, Palaeoclimatology, Palaeoecology, 271,* 170-181.

Hu, J., D. J. P. Moore, S. P. Burns, and R. K. Monson, (2010), Longer growing seasons lead to less carbon sequestration by a subalpine forest, *Global Change Biology, 16*, 771-783.

Kapp, R.O., Davis, O.K. and King, J.E., 2000. Pollen and spores, The American Association of Stratigraphic Palynologists 2nd Edition. Texas A&M University, College Station, Texas, USA.

Kershaw, L., MacKinnon, A., and Pojar, J., 1998. *Plants of the Rocky Mountains.* Lone Pine Publishing, Edmonton, AB, Canada.

Kelly, R.L., T.A. Surovell, B.N. Shuman, and G.M. Smith, (2013), A continuous climatic impact on Holocene human population in the Rocky Mountains, *Proceedings of the National Academy of Sciences, 110*(2), pp.443-447.

Krause, T.R. and C. Whitlock, (2013), Climate and vegetation change during the late-glacial/early-Holocene transition inferred from multiple proxy records from Blacktail Pond, Yellowstone National Park, USA, *Quaternary Research, 79,* 391-402.

Krause, T.R., Y. Lu, C. Whitlock, S.C. Fritz, and K.L. Pierce, (2015), Patterns of terrestrial and limnologic development in the northern Greater Yellowstone Ecosystem (USA) during the late-glacial/early-Holocene transition, *Palaeogeography, Palaeoclimatology, Palaeoecology, 422,* pp.46-56.

Kuehn, S.C., D.G., Froese, P.E., Carrara, F.F. Franklin Jr., N.J.G., Pearce, and P. Rotheisler, (2009), Major-and trace-element characterization, expanded distribution, and a new chronology for the latest Pleistocene Glacier Peak tephras in western North America, *Quaternary Research, 71,* pp.201-216.

Li, F., J. Sun, Y. Zhao, X. Guo, W. Zhao, and K. Zhang, (2010), Ecological significance of common pollen ratios: A review, *Frontiers in Earth Sciences China, 4*(3), pp.253-258.

Licciardi, J.M., and K. L., Pierce, (2008), Cosmogenic exposure-age chronologies of Pinedale and Bull Lake glaciations in greater Yellowstone and the Teton Range, USA, *Quaternary Science Reviews, 27,* 814-831.

Licciardi, J.M., P.U. Clark, E.J. Brook, D. Elmore, and S. Pankaj, (2004), Variable responses of western U.S. glaciers during the last deglaciation, *Geology, 32*(1).

MacDonald, D.H., 2012. *Montana Before History.* Mountain Press Publishing Company, Missoula, Montana.

McMannis, W.J., (1955), Geology of the Bridger Range, Montana, *Bulletin of the Geological Society of America, 66*, 1385-1430.

McWethy, D.B., C. Whitlock, J.M. Wilmshurst, M.S. McGlone, M. Fromont, X. Li, A. Dieffenbacher-Krall, W.O. Hobbs, S.C. Fritz, and E. R. Cook, (2010), Rapid landscape transformation in South Island, New Zealand, following initial Polynesian settlement, *Proceeding of the National Academy of Sciences, 107*(50), 21343-21348.

Mensing, S.A., L.V. Benson, M. Kashgarian, and S. Lund, (2004), A Holocene pollen record of persistent droughts from Pyramid Lake, Nevada, USA, *Quaternary Research, 62,* pp.29-38.

Meyer, G.A., S.G., Wells, and A.J., Timothy Jull, (1995), Fire and alluvial chronology in Yellowstone National Park: Climatic and intrinsic controls on Holocene geomorphic processes, *GSA Bulletin, 107*(10), pp.1211-1230.

Millspaugh, S.H., Whitlock, C., and Bartlein, P.J., 2004. Postglacial Fire, Vegetation, and Climate History of the Yellowstone-Lamar and Central Plateau Provinces, Yellowstone National Park. In Wallace, L.L. (Ed), *After the Fires: The Ecology of Change in Yellowstone National Park.* New Haven and London:Yale University Press. pp. 10-28.

Millspaugh, S.H., C. Whitlock, and P.J. Bartlein, (2000), Variations in fire frequency and climate over the past 17,000 yr in central Yellowstone National Park, *Geology, 28*(3), 211-214.

Millspaugh, S.H., C. Whitlock, (1995), A 750-year fire history based on lake sediment records in central Yellowstone National Park, USA, *The Holocene, 5*(3), pp. 283-292.

McAndrews, J.H., Berti, A.A., and Norris, G. 1973. Key to the Quaternary Pollen and Spores of the Great Lakes Region. Life Sci. Misc. Publ., Royal Ontario Museum.

Mock, C.J., (1996), Climatic Controls and Spatial Variations of Precipitation in the Western United States, *Journal of Climate*, *9, pp.*1111-1125.

Moore, P.O., and Webb, J.A., 1978. An Illustrated Guide to Pollen Analysis. John Wiley and Sons, New York, USA.

Mumma, S.A., C. Whitlock, and K. Pierce, (2012), A 28,000 year history of vegetation and climate from Lower Red Rock Lake, Centennial Valley, Southwestern Montana, USA, *Palaeogeography, Palaeoclimatology, Palaeoecology, 326-328.* pp.30-41.

National Park Service, (2016), Yellowstone Resources and Issues Handbook, *Greater Yellowstone Ecosystem.* Retrieved June 2016 from https://www.nps.gov/yell/learn/resources-and-issues.htm.

Neotomadb.org (2016), Neotoma Paleoecology Database.

North Central Climate Science Center (2016), North Central Climate Science Center Paleoecology Database, http://www.nccscpaleoenvironmentaldatabase.com.

Pablo, M., (2014), *Personal communication,* recorded during an in-person interview, Jan., 2014.

Persico, L., and G. Meyer, (2009), Holocene beaver damming, fluvial geomorphology, and climate in Yellowstone National Park, Wyoming, *Quaternary Research, 71*, pp.340-353.

Pfister, R.D., B.L., Kovalchik, S.F. Arno, and R.C. Presby, (1977), Forest Habitat Types of Montana, USDA Forest Service General Technical Report INT-34.

Pierce, K.L., (2015), *Personal communication,* recorded during an in-person interview, Sept., 2015.

Power, M. J., J. Marlon, N. Ortiz, P. J. Bartlein, S. P. Harrison, F. E. Mayle, A. Ballouche, R. H. W. Bradshaw, C. Carcaillet, C. Cordova, S. Mooney, P. I. Moreno, I. C. Prentice, K. Thonicke, W. Tinner, C. Whitlock, Y. Zhang, Y. Zhao, A. A. Ali, R. S. Anderson, R. Beer, H. Behling, C. Briles, K. J. Brown, A. Brunelle, M. Bush, P. Camill, G. Q. Chu, J. Clark, D. Colombaroli, S. Connor, A.-L. Daniau, M. Daniels, J. Dodson, E. Doughty, M. E. Edwards, W. Finsinger, D. Foster, J. Frechette, M.-J. Gaillard, D. G. Gavin, E. Gobet, S. Haberle, D. J. Hallett, P. Higuera, G. Hope, S. Horn, J. Inoue, P. Kaltenrieder, L. Kennedy, Z. C. Kong, C. Larsen, C. J. Long, J. Lynch, E. A. Lynch, M. McGlone, S. Meeks, S. Mensing, G. Meyer, T. Minckley, J. Mohr, D. M. Nelson, J. New, R. Newnham, R. Noti, W. Oswald, J. Pierce, P. J. H. Richard, C. Rowe, M. F. Sanchez Goñi, B. N. Shuman, H. Takahara, J. Toney, C. Turney, D. H. Urrego-Sanchez, C. Umbanhowar, M. Vandergoes, B. Vanniere, E. Vescovi, M. Walsh, X. Wang, N. Williams, J. Wilmshurst, and J. H. Zhang., (2008), Changes in fire regimes since the Last Glacial Maximum: an assessment based on a global synthesis and analysis of charcoal data, *Climate Dynamics 30*, pp.887–907.

Power, M.J., C. Whitlock, and P.J. Bartlein, (2011), Postglacial fire, vegetation, and climate history across an elevational gradient in the Northern Rocky Mountains, USA, and Canada, *Quaternary Science Reviews, 30*, 19-20, pp.2520-2533.

PRISM Climate Group, (2015), Oregon State University, http://prism.oregonstate.edu, created 4 Feb 2004.

Rasmussen, M., S.L. Anzick, M.R. Waters, P. Skoglund, M. DeGiorgio, T.W. Stafford Jr., S. Rasmussen, I. Moltke, A. Albrechtsen, S.M. Doyle, G.D. Poznik, V. Gudmundsdottir, R. Yadav, A. Malaspinas, S. Stockton Whit V, M.E. Allentoft, O.E. Cornejo, K. Tambets, A. Eriksson, P.D. Heintzman, M. Karmin, T.S. Korneiliussen, D.J. Meltzer, T.L. Pierre, J. Stenderup, L. Saag, V.M. Warmuth, M.C. Lopes, R.S. Malhi, S. Brunak, T. Sicheritz-Ponten, I. Barnes, M. Collins, L. Orlando, F. Balloux, A. Manica, R. Gupta, M. Metspalu, C.D. Bustamante, M. Jakobsson, R. Nielsen, and E. Willerslev, (2014), The genome of a Late Pleistocene human from a Clovis burial site in western Montana. *Nature*, *506*(7487), pp.225-229.

Reasoner, M.A., G., Osborn, and N.W. Rutter, (1994), Age of the Crowfoot advance in the Canadian Rocky Mountains: A glacial event coeval with the Younger Dryas oscillation, *Geology, 22,* pp.439-442.

Reimer, P.J., E. Bard, A. Bayliss, J.W. Beck, P.G. Blackwell, C. Bronk Ramsey, C.E. Buck, R.L. Edwards, M. Friedrich, P.M. Grootes, T.P. Guilderson, H. Haflidason, I. Hajdas, C. Hatté, T.J. Heaton, D.L. Hoffmann, A.G. Hogg, K.A. Hughen, K.F. Kaiser, B. Kromer, S.W. Manning, M. Niu, R.W. Reimer, D.A. Richards, E.M. Scott, J.R. Southon, C.S.M. Turney, J. van der Plicht, (2013), IntCal13 and Marine13 radiocarbon age calibration curves, 0-50,000 years cal BP, *Radiocarbon 55*, pp.1869-1887.

Roberts, D., (2016), *Personal communication,* recorded from an email conversation, Apr., 2016.

Schoennagel, T., T.T. Veblen, and W.H. Romme, (2004), The Interaction of Fire, Fuels, and Climate across Rocky Mountain Forests, *BioScience, 54*(7), pp.661-672.

Shinker, J.J., P.J. Bartlein, B. Shuman, (2006), Synoptic and dynamic climate controls of North American mid-continental aridity, *Quaternary Science Reviews, 25,* pp. 1401-1417.

Shinker, J.J. (2010), Visualizing Spatial Heterogeneity of Western U.S. Climate Variability, *Earth Interactions, 14*(10), pp.1-15.

Shuman, B., P. Pribyl, T.A. Minckley, and J.J. Shinker, (2010), Rapid hydrologic shifts and prolonged droughts in Rocky Mountain headwaters during the Holocene, *Geophysical Research Letters, 37.*

Thompson, R. S., K.H. Anderson, R.T. Pelltier, S.L. Shafer, and P.J. Bartlein, (2007), Atlas of Relations Between Climatic Parameters and Distributions of Important Trees and Shrubs in North America – Ecoregions fo North America, *U.S. Geological Survey, Professional Paper, 1650-E*.

Trujillo, E., N. P. Molotch, M. L. Goulden, A. E. Kelly, and R. C. Bales, (2012), Elevation-dependent influence of snow accumulation on forest greening, *Nature Geoscience, 1571*, pp. 1-5.

Waddington, J.C.B., and H.E. Wright Jr., (1974), Late Quaternary Vegetational Changes on the East Side of Yellowstone Park, Wyoming. *Quaternary Research. 4.* 175-184.

Western Regional Climate Center, (2016), Western U.S. Climate Summaries – NOAA coop stations, retrieved June 2016, from http://www.wrcc.dri.edu/climate-summaries/.

Whitlock, C. (1993), Postglacial Vegetation and Climate of Grand Teton and Southern Yellowstone National Parks, *Ecological Monographs. 63*(2), pp.173-198.

Whitlock, C., and P.J. Bartlein, (1993), Spatial Variations of Holocene Climatic Change in the Yellowstone Region, *Quaternary Research, 39.* pp.231-238.

Whitlock, C. and Larsen, C. 2001. Charcoal as fire proxy. In: Smol, J.P., Birks, H.J.B., Last, W.M. (Eds.), Tracking Environmental Change Using Lake Sediments. Terrestrial, Algal, and Siliceous Indicators, 3. Kluwer Academic Publishers, Dordrecht.

Whitlock, C. and Knox, M. 2002. Prehistoric Burning in the Pacific Northwest: Human versus Climatic Influences. In: Vale, T.R. (Ed.), Fire, Native Peoples, and The Natural Landscape. Island Press, Washington D.C.

Whitlock, C., W. Dean, J. Rosenbaum, L. Stevens, S. Fritz, B. Bracht, M. Power, (2007), A 2650-year long record of environmental change from northern Yellowstone National Park based on comparison of multiple proxy data, *Quaternary International.*

Whitlock, C., J. Marlon, C. Briles, a. Brunelle, C. Long, and P. Bartlein, (2008), Long-term relations among fire, fuel, and climate in the north-western US based on lake-sediment studies, *International Journal of Wildland Fire, 17*, pp.72-83.

Whitlock, C., W.E. Dean, S.C. Fritz, L.R. Stevens, J.R. Stone, M.J. Power, J.R. Rosenbaum, K.L. Pierce, B.B. Bracht-Flyr, (2012), Holocene seasonal variability inferred from multiple proxy records from Crevice lake, Yellowstone National Park, USA, *Palaeogeography, Palaeoclimatology, Palaeoecology, 331-332*, 90-103.

Wigand, P.E., (1987), Diamond Pond, Harney County, Oregon: Vegetation History and Water Table in the Eastern Oregon Desert, *The Great Basin Naturalist, 47*(3), pp.427-458.

Wright Jr., H.E., D.H. Mann, P.H. Glaser, (1983), Piston corers for peat and lake sediments, *Ecology, 65*. pp.657-659.

APPENDICES

APPENDIX A

RAW CHARCOAL COUNTS

Age (cal yr BP)	Sediment Depth (cm)	Charcoal Counts (# particles)	Sediment Volume (cm^3)
748	50	13	0.25
756	50.5	26	1.75
763	51	28	2
770	51.5	22	2
778	52	13	2
785	52.5	8	2
793	53	5	1.75
800	53.5	0	2
807	54	1	1.75
815	54.5	2	2
822	55	2	2
829	55.5	2	2
837	56	7	2
844	56.5	4	2
851	57	4	2
859	57.5	5	2
866	58	1	2
873	58.5	3	2
880	59	0	2
887	59.5	3	2
895	60	3	2
902	60.5	2	2
909	61	4	2
916	61.5	3	2
923	62	10	2
923	62.5	6	2
923	63	12	2
923	63.5	1	2
923	64	0	2
930	64.5	3	2
937	65	5	2
944	65.5	6	2
951	66	14	2
958	66.5	11	2
965	67	12	2
972	67.5	14	2

Age (cal yr BP)	Sediment Depth (cm)	Charcoal Counts (# particles)	Sediment Volume (cm^3)
979	68	9	2
986	68.5	10	2
993	69	12	2
1000	69.5	15	2
1014	70.5	4	2
1021	71	5	2
1027	71.5	12	2
1034	72	15	2
1041	72.5	25	2
1048	73	17	2
1055	73.5	9	2
1061	74	12	2
1068	74.5	15	2
1075	75	19	2
1081	75.5	30	2
1088	76	16	2
1095	76.5	9	2
1101	77	6	2
1108	77.5	2	2
1114	78	7	2
1121	78.5	7	2
1127	79	22	2
1134	79.5	10	2
1140	80	13	2
1147	80.5	28	2
1153	81	22	2
1160	81.5	120	2
1166	82	90	2
1172	82.5	6	2
1179	83	20	2
1185	83.5	8	2
1191	84	11	2
1198	84.5	9	2
1204	85	9	2
1210	85.5	19	2
1216	86	14	2

1223	86.5	4	2
1229	87	2	2
1235	87.5	4	2
1241	88	5	2
1247	88.5	2	2
1253	89	11	2
1259	89.5	13	2
1266	90	23	2
Age (cal yr BP)	Sediment Depth (cm)	Charcoal Counts (# particles)	Sediment Volume (cm^3)
1278	91	17	2
1284	91.5	11	2
1290	92	21	2
1296	92.5	26	2
1302	93	26	2
1308	93.5	38	2
1314	94	39	2
1320	94.5	50	2
1326	95	40	2
1332	95.5	27	2
1338	96	28	2
1343	96.5	9	2
1349	97	10	2
1355	97.5	19	2
1361	98	36	2
1367	98.5	27	2
1373	99	18	2
1379	99.5	17	2
1385	100	22	2
1390	100.5	15	2
1396	101	3	2
1402	101.5	5	2
1408	102	6	2
1413	102.5	22	2
1419	103	20	2
1425	103.5	18	2
1431	104	16	2
1436	104.5	14	2

1442	105	15	2
1448	105.5	6	2
1454	106	22	2
1459	106.5	17	2
1465	107	4	2
1471	107.5	19	2
1476	108	14	2
1482	108.5	15	2
1488	109	17	2
1493	109.5	20	2
1499	110	27	2
1504	110.5	9	2
Age (cal yr BP)	Sediment Depth (cm)	Charcoal Counts (# particles)	Sediment Volume (cm^3)
1516	111.5	5	2
1521	112	12	2
1527	112.5	34	2
1533	113	12	2
1538	113.5	9	2
1544	114	18	2
1549	114.5	5	2
1555	115	10	2
1560	115.5	27	2
1566	116	22	2
1572	116.5	20	2
1577	117	24	2
1583	117.5	4	2
1588	118	26	2
1594	118.5	7	2
1599	119	81	2
1605	119.5	87	2
1610	120	17	2
1616	120.5	40	2
1622	121	82	2
1627	121.5	424	2
1633	122	50	2
1638	122.5	40	2
1644	123	25	2

1649	123.5	8	2
1655	124	17	2
1660	124.5	17	2
1666	125	13	2
1671	125.5	13	2
1677	126	16	2
1682	126.5	22	2
1688	127	9	2
1694	127.5	7	2
1699	128	13	2
1705	128.5	5	2
1710	129	11	2
1716	129.5	8	2
1721	130	12	2
1727	130.5	11	2
1733	131	5	2
Age (cal yr BP)	Sediment Depth (cm)	Charcoal Counts (# particles)	Sediment Volume (cm^3)
1744	132	6	2
1749	132.5	11	2
1755	133	3	2
1761	133.5	8	2
1766	134	1	2
1772	134.5	2	2
1778	135	0	2
1784	135.5	1	2
1789	136	3	2
1795	136.5	16	2
1801	137	6	2
1807	137.5	16	2
1812	138	11	2
1818	138.5	4	2
1824	139	15	2
1830	139.5	23	2
1836	140	15	2
1842	140.5	2	2
1848	141	5	2
1853	141.5	3	2

1859	142	2	2
1865	142.5	0	2
1871	143	7	2
1877	143.5	4	2
1883	144	9	2
1889	144.5	9	2
1896	145	15	2
1902	145.5	6	2
1908	146	0	2
1914	146.5	0	0
1920	147	0	0
1926	147.5	0	0
1933	148	0	0
1939	148.5	0	0
1945	149	0	0
1952	149.5	0	0
1958	150	19	2
1964	150.5	11	2
1971	151	24	2
1977	151.5	19	2

Age (cal yr BP)	Sediment Depth (cm)	Charcoal Counts (# particles)	Sediment Volume (cm^3)
1990	152.5	22	2
1997	153	20	2
2004	153.5	15	2
2010	154	16	2
2017	154.5	14	2
2024	155	15	2
2030	155.5	14	2
2037	156	29	2
2044	156.5	56	2
2051	157	58	2
2058	157.5	21	2
2065	158	11	2
2072	158.5	16	2
2079	159	25	2
2086	159.5	25	2
2093	160	16	2

2100	160.5	16	2
2107	161	15	2
2115	161.5	16	2
2122	162	14	2
2129	162.5	14	2
2137	163	11	2
2144	163.5	21	2
2152	164	11	2
2159	164.5	23	2
2167	165	40	2
2174	165.5	41	2
2182	166	77	2
2190	166.5	23	2
2198	167	21	2
2206	167.5	12	2
2213	168	4	2
2221	168.5	3	2
2229	169	10	2
2237	169.5	15	2
2246	170	16	2
2254	170.5	11	2
2262	171	2	2
2270	171.5	4	2
2279	172	2	2

Age (cal yr BP)	Sediment Depth (cm)	Charcoal Counts (# particles)	Sediment Volume (cm^3)
2295	173	8	2
2304	173.5	11	2
2313	174	16	2
2321	174.5	16	2
2330	175	26	2
2339	175.5	51	2
2347	176	7	2
2356	176.5	8	2
2365	177	7	2
2374	177.5	3	2
2383	178	11	2
2392	178.5	9	2

2402	179	13	2
2411	179.5	3	2
2420	180	2	2
2430	180.5	15	2
2439	181	14	2
2449	181.5	6	2
2458	182	15	2
2468	182.5	8	2
2478	183	6	2
2487	183.5	9	2
2497	184	6	2
2507	184.5	16	2
2517	185	12	2
2527	185.5	5	2
2537	186	13	2
2547	186.5	10	2
2558	187	7	2
2568	187.5	1	2
2579	188	0	2
2589	188.5	3	2
2600	189	10	2
2610	189.5	13	2
2621	190	19	2
2632	190.5	21	2
2642	191	27	2
2653	191.5	33	2
2664	192	7	2
2675	192.5	9	2

Age (cal yr BP)	Sediment Depth (cm)	Charcoal Counts (# particles)	Sediment Volume (cm^3)
2698	193.5	100	2
2709	194	39	2
2720	194.5	3	2
2732	195	1	2
2743	195.5	11	2
2755	196	14	2
2766	196.5	10	2
2778	197	9	2

2790	197.5	6	2
2802	198	8	2
2813	198.5	10	2
2825	199	12	2
2838	199.5	25	2
2850	200	13	2
2862	200.5	10	2
2874	201	8	2
2887	201.5	7	2
2899	202	24	2
2912	202.5	16	2
2924	203	17	2
2937	203.5	2	2
2950	204	5	2
2962	204.5	22	2
2975	205	10	2
2988	205.5	11	2
3001	206	13	2
3014	206.5	16	2
3028	207	18	2
3041	207.5	8	2
3054	208	17	2
3068	208.5	23	2
3081	209	10	2
3095	209.5	15	2
3109	210	40	2
3122	210.5	52	2
3136	211	33	2
3150	211.5	17	2
3164	212	9	2
3178	212.5	6	2
3192	213	6	2
Age (cal yr BP)	Sediment Depth (cm)	Charcoal Counts (# particles)	Sediment Volume (cm^3)
3221	214	14	2
3235	214.5	12	2
3249	215	30	2
3264	215.5	10	2

3278	216	8	2
3293	216.5	34	2
3308	217	22	2
3322	217.5	37	2
3337	218	103	2
3352	218.5	24	2
3367	219	43	2
3382	219.5	24	2
3397	220	12	2
3412	220.5	11	2
3428	221	23	2
3443	221.5	38	2
3458	222	17	2
3474	222.5	9	2
3489	223	4	2
3505	223.5	18	2
3521	224	30	2
3536	224.5	18	2
3552	225	24	2
3568	225.5	12	2
3584	226	20	2
3600	226.5	8	2
3616	227	12	2
3632	227.5	9	2
3648	228	3	2
3664	228.5	0	2
3681	229	20	2
3697	229.5	14	2
3713	230	24	2
3730	230.5	11	2
3747	231	7	2
3763	231.5	12	2
3780	232	8	2
3797	232.5	5	2
3813	233	10	2
3830	233.5	19	2
Age (cal yr BP)	Sediment Depth (cm)	Charcoal Counts (# particles)	Sediment Volume (cm^3)

3864	234.5	14	2
3881	235	8	2
3898	235.5	3	2
3915	236	9	2
3933	236.5	16	2
3950	237	11	2
3967	237.5	32	2
3985	238	31	2
4002	238.5	21	2
4020	239	7	2
4037	239.5	13	2
4055	240	22	2
4073	240.5	11	2
4090	241	6	2
4108	241.5	12	2
4126	242	18	2
4144	242.5	26	2
4162	243	18	2
4180	243.5	27	2
4198	244	32	2
4216	244.5	10	2
4234	245	10	2
4253	245.5	16	2
4271	246	7	2
4289	246.5	0	0
4308	247	0	0
4326	247.5	0	0
4345	248	0	0
4363	248.5	0	0
4382	249	0	0
4400	249.5	0	0
4419	250	12	1.75
4438	250.5	21	1.75
4457	251	31	2
4476	251.5	65	2
4494	252	85	2
4513	252.5	58	2
4532	253	40	2
4551	253.5	26	2

4571	254	27	2
Age (cal yr BP)	Sediment Depth (cm)	Charcoal Counts (# particles)	Sediment Volume (cm^3)
4609	255	11	2
4628	255.5	21	2
4648	256	9	2
4667	256.5	18	2
4686	257	15	2
4706	257.5	10	2
4725	258	24	2
4745	258.5	11	2
4764	259	9	2
4784	259.5	8	2
4804	260	21	2
4823	260.5	7	2
4843	261	5	2
4863	261.5	17	2
4883	262	5	2
4903	262.5	11	2
4923	263	10	2
4943	263.5	20	2
4963	264	14	2
4983	264.5	22	2
5003	265	44	2
5023	265.5	22	2
5043	266	7	2
5064	266.5	13	2
5084	267	10	2
5104	267.5	4	2
5125	268	13	2
5145	268.5	7	2
5165	269	7	2
5186	269.5	7	2
5206	270	11	2
5227	270.5	12	2
5248	271	14	2
5268	271.5	5	2
5289	272	12	2

Age (cal yr BP)	Sediment Depth (cm)	Charcoal Counts (# particles)	Sediment Volume (cm^3)
5310	272.5	14	2
5330	273	5	2
5351	273.5	1	2
5372	274	0	2
5393	274.5	17	2
5435	275.5	4	2
5456	276	23	2
5477	276.5	30	2
5498	277	4	2
5519	277.5	0	2
5540	278	2	2
5562	278.5	3	2
5583	279	0	2
5604	279.5	0	2
5626	280	1	2
5647	280.5	2	2
5668	281	0	2
5690	281.5	1	2
5711	282	0	2
5733	282.5	0	2
5755	283	0	2
5776	283.5	0	2
5798	284	1	2
5820	284.5	2	2
5841	285	0	2
5863	285.5	1	2
5885	286	3	2
5907	286.5	1	2
5929	287	2	2
5951	287.5	6	2
5973	288	1	2
5995	288.5	4	2
6017	289	1	2
6040	289.5	5	2
6062	290	0	2
6084	290.5	0	2

6107	291	7	2
6129	291.5	3	2
6151	292	5	2
6174	292.5	10	2
6196	293	2	2
6219	293.5	13	2
6242	294	7	2
6264	294.5	5	2
6287	295	9	2
Age (cal yr BP)	Sediment Depth (cm)	Charcoal Counts (# particles)	Sediment Volume (cm^3)
6333	296	15	2
6356	296.5	11	2
6379	297	29	2
6402	297.5	50	2
6425	298	29	2
6448	298.5	16	2
6471	299	14	2
6494	299.5	16	2
6517	300	19	2
6541	300.5	17	2
6564	301	6	2
6587	301.5	31	2
6611	302	9	2
6634	302.5	25	2
6658	303	13	2
6681	303.5	8	2
6705	304	20	2
6729	304.5	2	2
6752	305	12	2
6776	305.5	5	2
6800	306	17	2
6824	306.5	10	2
6848	307	13	2
6872	307.5	16	2
6896	308	11	2
6920	308.5	21	2
6944	309	24	2

6968	309.5	19	2
6992	310	16	2
7017	310.5	6	2
7041	311	6	2
7065	311.5	4	2
7090	312	1	2
7114	312.5	17	2
7139	313	12	2
7163	313.5	11	2
7188	314	12	2
7212	314.5	28	2
7237	315	14	2
7262	315.5	5	2
Age (cal yr BP)	Sediment Depth (cm)	Charcoal Counts (# particles)	Sediment Volume (cm^3)
7311	316.5	25	2
7336	317	10	2
7361	317.5	0	2
7386	318	13	2
7410	318.5	8	2
7435	319	3	2
7460	319.5	7	2
7485	320	1	2
7510	320.5	1	2
7535	321	4	2
7561	321.5	10	2
7586	322	6	2
7611	322.5	13	2
7636	323	21	2
7661	323.5	0	2
7687	324	10	2
7712	324.5	37	2
7737	325	10	2
7762	325.5	5	2
7788	326	2	2
7813	326.5	13	2
7839	327	3	2
7864	327.5	11	2

7890	328	8	2
7915	328.5	8	2
7941	329	23	2
7966	329.5	9	2
7992	330	28	2
8017	330.5	13	2
8043	331	13	2
8069	331.5	16	2
8094	332	11	2
8120	332.5	6	2
8146	333	1	2
8172	333.5	0	2
8197	334	9	2
8223	334.5	10	2
8249	335	6	2
8275	335.5	17	2
8301	336	5	2
Age (cal yr BP)	Sediment Depth (cm)	Charcoal Counts (# particles)	Sediment Volume (cm^3)
8352	337	24	2
8378	337.5	12	2
8404	338	9	2
8430	338.5	11	2
8456	339	27	2
8482	339.5	29	2
8508	340	14	2
8534	340.5	14	2
8559	341	12	2
8585	341.5	18	2
8611	342	9	2
8637	342.5	5	2
8663	343	14	2
8689	343.5	10	2
8715	344	8	2
8741	344.5	42	2
8767	345	0	2
8792	345.5	12	2
8818	346	14	2

8844	346.5	14	2
8870	347	21	2
8896	347.5	14	2
8921	348	10	2
8947	348.5	13	2
8973	349	14	2
8998	349.5	22	2
9024	350	10	0.75
9050	350.5	24	2
9075	351	22	2
9101	351.5	23	2
9126	352	7	2
9152	352.5	10	2
9177	353	17	2
9203	353.5	17	2
9228	354	16	2
9254	354.5	3	2
9279	355	16	2
9304	355.5	5	2
9330	356	8	2
9355	356.5	11	2

Age (cal yr BP)	Sediment Depth (cm)	Charcoal Counts (# particles)	Sediment Volume (cm^3)
9405	357.5	15	2
9430	358	14	2
9455	358.5	8	2
9480	359	20	2
9505	359.5	22	2
9530	360	23	2
9555	360.5	9	2
9579	361	14	2
9604	361.5	10	2
9629	362	13	2
9653	362.5	17	2
9678	363	22	2
9702	363.5	41	2
9727	364	29	2
9751	364.5	24	2

9775	365	16	2
9799	365.5	37	2
9823	366	15	2
9847	366.5	11	2
9871	367	15	2
9895	367.5	23	2
9919	368	14	2
9943	368.5	6	2
9967	369	31	2
9990	369.5	18	2
10014	370	32	2
10037	370.5	16	2
10061	371	23	2
10084	371.5	15	2
10108	372	45	2
10131	372.5	24	2
10154	373	19	2
10177	373.5	17	2
10200	374	45	2
10223	374.5	22	2
10246	375	73	2
10269	375.5	34	2
10292	376	45	2
10315	376.5	139	2
10338	377	76	2

Age (cal yr BP)	Sediment Depth (cm)	Charcoal Counts (# particles)	Sediment Volume (cm^3)
10383	378	20	2
10405	378.5	27	2
10428	379	20	2
10450	379.5	5	2
10473	380	8	2
10495	380.5	2	2
10517	381	10	2
10539	381.5	9	2
10562	382	1	2
10584	382.5	32	2
10606	383	38	2

10628	383.5	32	2
10650	384	17	2
10671	384.5	0	2
10693	385	14	2
10715	385.5	33	2
10737	386	24	2
10758	386.5	17	2
10780	387	9	2
10801	387.5	5	2
10823	388	2	2
10844	388.5	3	2
10866	389	6	2
10887	389.5	2	2
10908	390	1	2
10930	390.5	10	2
10951	391	2	2
10972	391.5	26	2
10993	392	6	2
11014	392.5	4	2
11035	393	4	2
11056	393.5	3	2
11077	394	6	2
11098	394.5	4	2
11118	395	2	2
11139	395.5	3	2
11160	396	1	2
11181	396.5	0	2
11201	397	0	2
11222	397.5	0	2

Age (cal yr BP)	Sediment Depth (cm)	Charcoal Counts (# particles)	Sediment Volume (cm^3)
11263	398.5	0	2
11283	399	0	2
11304	399.5	1	2
11324	400	0	2
11344	400.5	1	2
11364	401	0	2
11385	401.5	1	2

Age (cal yr BP)	Sediment Depth (cm)	Charcoal Counts (# particles)	Sediment Volume (cm^3)
11405	402	0	2
11405	402.5	0	2
11405	403	0	2
11405	403.5	0	2
11405	404	0	2
11405	404.5	0	2
11405	405	1	2
11405	405.5	0	2
11405	406	0	2
11405	406.5	0	2
11405	407	1	2
11405	407.5	0	2
11405	408	12	2
11405	408.5	0	2
11405	409	0	2
11405	409.5	0	2
11405	410	0	1.75
11405	410.5	0	2
11425	411	0	2
11445	411.5	1	2
11465	412	0	2
11485	412.5	0	2
11505	413	0	2
11525	413.5	0	2
11545	414	1	2
11565	414.5	2	2
11584	415	0	2
11604	415.5	4	2
11624	416	1	2
11644	416.5	0	2
11644	417	0	2
11644	417.5	0	2
11644	418	0	2
11644	419	1	2
11644	419.5	0	2
11644	420	3	2

11663	420.5	0	2
11683	421	2	2
11702	421.5	3	2
11722	422	0	2
11741	422.5	0	2
11761	423	0	1
11780	423.5	0	2
11800	424	0	2
11819	424.5	0	2
11838	425	1	2
11858	425.5	1	2
11877	426	1	2
11896	426.5	0	2
11915	427	2	2
11934	427.5	0	2
11953	428	0	2
11972	428.5	0	2
11991	429	0	2
12010	429.5	0	2
12029	430	0	2
12048	430.5	2	2
12067	431	0	2
12086	431.5	0	1.75
12105	432	1	2
12124	432.5	5	2
12143	433	3	2
12161	433.5	8	2
12180	434	17	2
12199	434.5	3	2
12218	435	7	2
12236	435.5	3	2
12255	436	13	2
12273	436.5	20	2
12292	437	56	2
12310	437.5	3	2
12329	438	34	2
12347	438.5	19	2

Age (cal yr BP)	Sediment Depth (cm)	Charcoal Counts (# particles)	Sediment Volume (cm^3)
12384	439.5	10	2
12403	440	4	2
12421	440.5	5	2
12439	441	4	2
12458	441.5	0	2
12476	442	0	2
12494	442.5	3	2
12513	443	8	2
12531	443.5	1	2
12549	444	2	2
12567	444.5	0	2
12585	445	4	2
12604	445.5	0	2
12622	446	0	2
12640	446.5	0	2
12658	447	7	2
12676	447.5	4	2
12694	448	1	2
12712	448.5	1	2
12730	449	2	2
12748	449.5	15	2
12766	450	2	1
12784	450.5	3	1.5
12802	451	2	2
12820	451.5	5	2
12838	452	2	2
12856	452.5	0	2
12873	453	1	2
12891	453.5	0	2
12909	454	1	2
12927	454.5	1	2
12945	455	5	2
12963	455.5	1	2
12980	456	1	2
12998	456.5	0	2
13016	457	0	2

13034	457.5	0	2
13051	458	0	2
13069	458.5	0	2
13087	459	0	2
Age (cal yr BP)	Sediment Depth (cm)	Charcoal Counts (# particles)	Sediment Volume (cm^3)
13122	460	0	2
13140	460.5	1	2
13157	461	3	2
13175	461.5	0	2
13193	462	1	2
13210	462.5	0	2
13228	463	0	2
13245	463.5	0	2
13263	464	0	2
13281	464.5	2	2
13298	465	0	2
13316	465.5	0	2
13333	466	2	2
13351	466.5	0	2
13368	467	0	2
13386	467.5	2	2
13404	468	0	2
13421	468.5	1	2
13439	469	1	2
13456	469.5	0	2
13474	470	0	2
13491	470.5	0	2
13509	471	1	2
13526	471.5	0	2
13544	472	0	2
13561	472.5	2	2
13579	473	0	2
13596	473.5	0	2
13614	474	0	2
13631	474.5	0	2
13648	475	0	2
13666	475.5	0	2

13683	476	0	2
13701	476.5	0	2
13718	477	1	2
13736	477.5	0	2
13753	478	0	2
13771	478.5	0	2
13788	479	0	2
13806	479.5	0	2

Age (cal yr BP)	Sediment Depth (cm)	Charcoal Counts (# particles)	Sediment Volume (cm^3)
13841	480.5	0	2
13858	481	0	2
13876	481.5	0	2
13893	482	0	2
13911	482.5	0	2
13928	483	0	2
13946	483.5	1	2
13963	484	0	2
13981	484.5	0	2
13998	485	0	2
14015	485.5	0	2
14033	486	0	2
14050	486.5	2	2
14068	487	0	2
14085	487.5	0	2
14103	488	0	2
14120	488.5	0	2
14138	489	0	2
14155	489.5	0	2
14173	490	0	2
14190	490.5	0	2
14208	491	0	2
14225	491.5	0	2
14243	492	1	2
14260	492.5	1	2
14278	493	0	2
14295	493.5	0	2
14313	494	0	2

14330	494.5	0	2
14348	495	0	2
14365	495.5	0	2
14382	496	0	2
14400	496.5	0	2
14417	497	0	2
14435	497.5	0	2
14452	498	0	2
14470	498.5	0	2
14487	499	0	2
14505	499.5	0	2
14522	500	0	2
Age (cal yr BP)	Sediment Depth (cm)	Charcoal Counts (# particles)	Sediment Volume (cm^3)
14557	501	0	2
14575	501.5	0	2
14592	502	0	2
14610	502.5	0	2
14627	503	0	2
14645	503.5	0	2
14662	504	0	2
14680	504.5	1	2
14697	505	1	2
14715	505.5	2	2
14732	506	0	2
14749	506.5	0	2
14767	507	0	1.75
14784	507.5	0	2
14802	508	0	2
14819	508.5	0	2
14837	509	0	2
14854	509.5	3	2
14872	510	0	2
14889	510.5	0	2
14907	511	0	2
14924	511.5	1	2
14942	512	0	2
14959	512.5	0	2

Age (cal yr BP)	Sediment Depth (cm)	Charcoal Counts (# particles)	Sediment Volume (cm^3)
14977	513	1	2
14994	513.5	0	2
15012	514	1	2
15029	514.5	0	2
15047	515	0	2
15064	515.5	0	2
15082	516	1	2
15099	516.5	1	2
15116	517	0	2
15134	517.5	0	2
15151	518	0	2
15169	518.5	0	2
15186	519	0	2
15204	519.5	0	2
15221	520	0	2
15239	520.5	0	2
15274	521.5	1	2
15291	522	0	2
15309	522.5	0	2
15326	523	1	2
15344	523.5	0	2
15361	524	0	2
15379	524.5	0	2
15396	525	3	2
15414	525.5	0	2
15431	526	0	2
15449	526.5	0	2
15466	527	0	2
15483	527.5	0	2
15501	528	0	2
15518	528.5	1	2
15536	529	0	2
15553	529.5	0	2
15571	530	0	2
15588	530.5	0	2

15606	531	0	2
15623	531.5	0	2
15641	532	0	2
15658	532.5	2	2
15676	533	0	2
15693	533.5	0	2
15711	534	0	2
15728	534.5	0	2
15746	535	0	2
15763	535.5	0	2
15781	536	0	2
15798	536.5	0	2
15816	537	0	2
15833	537.5	0	2
15850	538	0	1.75
15868	538.5	0	2
15885	539	0	2
15903	539.5	0	2
15920	540	0	2

Age (cal yr BP)	Sediment Depth (cm)	Charcoal Counts (# particles)	Sediment Volume (cm^3)
15938	540.5	0	2
15955	541	0	2
15990	542	0	2
16008	542.5	0	2
16025	543	0	2
16043	543.5	0	2
16060	544	0	2
16078	544.5	0	2
16095	545	0	2
16113	545.5	1	2
16130	546	1	2
16148	546.5	2	2
16165	547	0	2
16183	547.5	4	1.5

APPENDIX B

POLLEN KEY

HAPLOXYLON	H
DIPLOXYLONJ	D
PINE	P
PICEA	I
ABIES	E
PSEUDOTSUGA	SU
CUPRESSACEAE	CU
ALNUS	AL
SALIX	S
POPULUS	PU
QUERCUS	Q
AMELANCHIER	AM
ACER GLABRUM	AG
SPIRAEA	RS
CEANOTHUS	CE
ARCETHOBIUM	AX
SARCOBATUS	SR
POACEAE	G
ARTEMISIA	R
TUBULIFLORAE	TU
LIGULIFLORAE	LG
AMARANTHACEAE	K
POLYGONUM TYPE	PG
BRASSICACEAE	BR
CORNUS	CR
ROSACEA	RO
BIDENS TYPE	BI
AMBROSIA	M
EPHEDRA	EF
BETULACEA	B
GALIUM	GA
UNKNOWN	Z
ONAGRACEAE	ON
RANUNCULACEA	RA
CARYOPHYLLACEAE	CF
FABACEAE	LE
THALICTRUM	TL
PTERIDIUM (BRAKEN FERN)	PT

PTERIDIUM UNDIFF	TER
INDETERMINATE	IN
WOODSIA	WO
RUMEX	RU
APIACEAE	AP
PRUNUS VIRGINIANA	PR
SHEPERDIA CANADENSIS	SC
DRYOPTERIS	DY
CYPERACEAE	Y

MYRIOPHYLLUM	MY
POTAMOGETON	UP
PEDIASTRUM SIMPLEX	PS
PEDIASTRUM DUPLEX	PD
EQUISETUM	EQ
UTRICULARIA	UT
SELAGINELLA	SD
TYPHA	TY
SPORORMIELLA	BAR
SPKIE	EU

APPENDIX C

RAW POLLEN COUNTS

Depth (cm)	Age (cal yr BP)	H	D	P	I	E	SU	CU
50	748	29.5	18	75	50.5	12	4	1
62	923	44	24.5	59	28.5	23	2	3
74	1088	27.5	42.5	90.5	12.5	31	3	0
90	1290	60	27.5	86	15.5	22.5	2	1
110	1521	44.5	14	53	31.5	17.5	3	3
126	1699	43	32	65	13.5	14.5	5	1
138	1836	40.5	37	90	12	22	0	1
146	1933	47.5	18.5	50.5	42	10.5	3	3
162	2152	42.5	35	69	9	24.5	4	2
170	2279	49	30.5	77	9.5	14.5	2	0
182	2497	41	14	57	59.5	18.5	2	2
194	2755	16.5	11.5	43.5	44	26	9	0
206	3054	33	18	65.5	13.5	20.5	2	4
214	3278	39	20.5	72.5	17.5	25	5	3
222	3521	31.5	18	47	8	14.5	4	2
230	3780	21	11	63	44	20	9	1
242	4198	33	20.5	75.5	10	16.5	8	1
250	4494	22	19	35.5	55	17.5	6	5
258	4804	22	17.5	71	21	27	11	2
262	4963	35.5	18	28	27.5	29.5	14	1
270	5289	45	15.5	88	20	25.5	21	0
278	5626	33	9	50.5	37.5	13.5	17	4
298	6517	30.5	10	51.5	21	13.5	7	1
302	6705	13	3	32.5	47.5	15.5	16	4
310	7090	36	19.5	69	6	12	13	1
318	7485	9	5	34.5	25.5	14.5	12	1
326	7890	56	26.5	74	10	24.5	6	4
330	8094	51	27	87	12.5	15	7	1
334	8301	50	25	65.5	11.5	16	20	1
342	8715	57	24	113.5	6.5	14.5	9	1
346	8921	19	14	83	10.5	13.5	2	0

350	9126	20.5	3	52	68.5	17	3	1
354	9330	15	5	46	88	23.5	0	1
362	9727	56	22.5	52.5	87	2	0	1
366	9919	32	8	48.5	142.5	33	0	0
370	10108	40	17	70.5	47.5	17	0	0
374	10292	24	9.5	46	87.5	11	0	2
378	10473	36.5	34	35	20.5	23.5	2	5
382	10650	5.5	5	44	35	33	1	2
386	10823	10.5	2	28	85.5	2	1	9
Depth (cm)	**Age (cal yr BP)**	**H**	**D**	**P**	**I**	**E**	**SU**	**CU**
390	10993	36	23.5	21	27.5	20	1	5
394	11160	38	41	55	40	9	0	4
398	11324	30.5	24.5	26.5	47.5	12.5	1	1
402	11485	46.5	46	39.5	10.5	5.5	0	2
410	11800	29	16.5	64.5	16	21.5	2	3
426	12403	4.5	8	9.5	17.5	11	0	3
434	12694	46.5	17.5	25.5	3.5	6.5	1	2
442	12980	30.5	27.5	30	8.5	2	1	7
446	13122	32	20	18.5	8.5	3	0	3
454	13404	25.5	31.5	27.5	9	6	0	4
462	13683	112	48.5	59.5	19	13	0	1
478	14243	19	5	7.5	32.5	2.5	0	1
486	14522	19.5	7	19	14	4.5	0	5
490	14662	22.5	31	29.5	4.5	11	0	1
506	15221	35	39	28	15.5	11	0	2
510	15361	33	22	45.5	1	2.5	0	3

Depth (cm)	**Age (cal yr BP)**	**AL**	**S**	**PU**	**Q**	**AM**	**AG**	**RS**
50	748	1	3	0	1	0	0	1
62	923	3	6	2	0	1	0	0
74	1088	2	0	6	0	0	1	0
90	1290	0	1	1	0	0	0	0
110	1521	5	3	0	0	0	0	0
126	1699	5	1	0	0	0	0	1
138	1836	2	2	2	0	0	0	0
146	1933	6	1	1	0	0	1	0

162	2152	3	0	1	0	0	0	0
170	2279	6	2	0	0	0	0	0
182	2497	4	0	1	0	0	1	0
194	2755	5	2	1	0	0	0	0
206	3054	8	3	0	0	0	0	0
214	3278	7	1	0	0	0	0	0
222	3521	8	2	0	1	1	0	0
230	3780	7	2	0	0	1	0	0
242	4198	3	0	1	0	1	0	0
250	4494	5	2	1	1	0	0	0
258	4804	3	0	0	1	0	4	0
262	4963	11	2	0	0	4	0	0
Depth (cm)	**Age (cal yr BP)**	**AL**	**S**	**PU**	**Q**	**AM**	**AG**	**RS**
270	5289	3	0	0	0	0	0	0
278	5626	5	3	1	0	0	0	0
298	6517	4	0	1	0	0	1	0
302	6705	3	4	0	1	1	0	0
310	7090	3	0	0	0	1	0	2
318	7485	7	4	1	1	0	0	0
326	7890	7	2	0	1	0	0	1
330	8094	2	1	0	0	0	1	0
334	8301	5	5	1	0	3	0	0
342	8715	1	2	0	0	0	0	0
346	8921	2	3	0	0	0	0	0
350	9126	4	0	0	1	0	1	0
354	9330	1	1	0	1	1	0	0
362	9727	1	2	0	1	1	0	0
366	9919	1	0	0	0	0	0	0
370	10108	0	1	0	0	0	0	0
374	10292	1	6	0	0	0	0	0
378	10473	3	8	2	0	1	0	0
382	10650	2	4	2	0	3	0	0
386	10823	4	9	0	0	0	0	0
390	10993	2	3	2	0	2	0	0
394	11160	5	9	6	0	2	0	0
398	11324	3	3	0	0	0	0	0
402	11485	4	2	2	0	3	0	1

410	11800	1	4	1	0	0	0	1
426	12403	8	2	4	0	0	0	0
434	12694	0	5	5	0	0	0	0
442	12980	10	7	1	0	0	0	1
446	13122	14	3	1	1	0	0	0
454	13404	6	8	1	1	2	0	0
462	13683	2	0	0	0	0	0	0
478	14243	6	9	16	1	0	1	0
486	14522	7	4	2	1	2	1	0
490	14662	0	1	0	0	0	0	0
506	15221	0	6	4	0	0	0	1
510	15361	4	9	2	0	1	0	3

Depth (cm)	**Age (cal yr BP)**	**CE**	**AX**	**SR**	**G**	**R**	**TU**	**LG**
50	748	3	0	2	29	42	7	0
62	923	0	0	2	41	47	3	0
74	1088	0	0	2	17	40	13	0
90	1290	0	1	8	34	22	1	0
110	1521	0	0	2	45	39	9	1
126	1699	2	0	6	43	44	3	0
138	1836	0	0	2	30	50	0	0
146	1933	0	0	2	33	48	9	0
162	2152	0	1	2	40	49	10	0
170	2279	0	0	3	24	47	1	0
182	2497	0	1	1	25	55	7	0
194	2755	0	0	4	43	67	16	1
206	3054	1	0	4	32	60	7	0
214	3278	0	0	6	23	53	4	0
222	3521	1	0	5	43	84	4	0
230	3780	0	0	0	31	64	5	0
242	4198	1	0	2	37	73	9	0
250	4494	1	0	1	27	69	9	1
258	4804	0	0	5	13	83	2	0
262	4963	0	0	3	38	67	11	0
270	5289	0	0	3	15	47	0	2

278	5626	0	0	2	24	54	3	0
298	6517	0	0	2	19	111	5	0
302	6705	2	0	2	25	94	6	0
310	7090	0	0	3	20	87	6	0
318	7485	0	1	4	33	97	9	1
326	7890	0	0	8	17	107	8	0
330	8094	0	0	5	21	55	2	0
334	8301	0	0	5	21	62	7	0
342	8715	0	0	7	15	53	4	0
346	8921	0	0	3	23	92	9	0
350	9126	0	0	6	15	90	8	1
354	9330	0	0	6	18	68	5	2
362	9727	1	0	1	17	35	3	2
366	9919	0	0	1	13	32	2	1
370	10108	0	0	5	16	80	6	1
374	10292	0	0	0	23	70	1	1
378	10473	0	0	1	28	73	3	0
382	10650	0	0	4	43	80	6	1
386	10823	0	0	0	35	84	4	1
Depth (cm)	**Age (cal yr BP)**	**CE**	**AX**	**SR**	**G**	**R**	**TU**	**LG**
390	10993	0	0	2	30	112	4	0
394	11160	0	0	0	41	95	4	1
398	11324	0	0	1	18	146	3	1
402	11485	0	0	0	16	116	3	1
410	11800	0	0	0	9	105	8	3
426	12403	1	0	4	20	167	7	0
434	12694	0	0	2	13	136	4	0
442	12980	0	0	1	40	135	6	1
446	13122	0	0	4	37	151	5	0
454	13404	0	0	1	30	116	5	1
462	13683	1	0	3	11	43	1	0
478	14243	1	0	1	23	130	5	0
486	14522	0	0	2	21	144	3	0
490	14662	0	1	3	14	138	8	0
506	15221	0	0	4	41	90	3	0
510	15361	0	0	8	31	98	9	0

Depth (cm)	Age (cal yr BP)	K	PG	BR	CR	RO	BI	M
50	748	12	0	1	0	3	1	1
62	923	11	0	2	0	0	0	3
74	1088	10	0	0	0	0	0	0
90	1290	7	0	1	0	0	0	5
110	1521	4	0	2	0	2	0	4
126	1699	6	0	0	0	3	0	3
138	1836	10	0	0	0	1	0	7
146	1933	14	1	0	0	3	0	2
162	2152	11	0	0	0	0	0	1
170	2279	14	0	0	0	1	1	13
182	2497	11	0	0	0	1	0	1
194	2755	10	0	0	0	0	1	4
206	3054	17	0	0	0	1	0	3
214	3278	13	0	0	0	0	2	1
222	3521	19	0	0	0	2	1	3
230	3780	15	1	0	0	0	0	6
242	4198	17	0	0	0	1	0	5
250	4494	22	0	0	0	1	1	4
258	4804	18	0	0	0	1	0	0
262	4963	27	0	1	0	1	1	6
Depth (cm)	**Age (cal yr BP)**	**K**	**PG**	**BR**	**CR**	**RO**	**BI**	**M**
270	5289	7	0	0	0	2	0	5
278	5626	26	0	1	0	1	1	5
298	6517	43	2	0	0	1	0	6
302	6705	24	1	0	0	1	0	1
310	7090	15	0	0	0	0	1	2
318	7485	36	0	0	0	0	0	5
326	7890	28	0	0	0	0	2	7
330	8094	35	0	0	0	1	0	10
334	8301	31	0	0	0	0	0	3
342	8715	27	0	0	0	2	1	3
346	8921	41	0	0	0	1	0	8
350	9126	31	1	1	0	0	0	6
354	9330	34	0	0	0	1	0	9
362	9727	25	0	0	0	1	0	8

366	9919	18	1	0	0	0	0	2
370	10108	15	0	0	0	1	0	3
374	10292	12	2	0	0	3	0	3
378	10473	11	0	0	0	1	0	3
382	10650	17	0	0	0	1	0	2
386	10823	9	5	0	0	3	0	0
390	10993	10	0	0	1	3	0	1
394	11160	8	0	0	0	0	0	2
398	11324	11	0	1	0	3	0	2
402	11485	7	0	1	0	1	0	1
410	11800	8	0	0	0	1	0	2
426	12403	28	0	0	0	0	0	1
434	12694	10	0	0	0	0	0	2
442	12980	14	0	3	0	1	0	1
446	13122	14	0	3	0	2	0	4
454	13404	6	0	0	0	2	0	5
462	13683	4	0	0	0	2	0	1
478	14243	9	0	0	0	4	0	0
486	14522	10	0	0	0	2	0	1
490	14662	13	0	0	0	2	1	1
506	15221	6	0	0	0	5	0	1
510	15361	4	1	0	0	1	0	3

Depth (cm)	**Age (cal yr BP)**	**EF**	**B**	**GA**	**Z**	**ON**	**RA**	**CF**
50	748	0	0	0	0	0	0	0
62	923	0	1	1	0	0	0	0
74	1088	0	0	0	0	0	0	1
90	1290	3	0	0	0	0	0	2
110	1521	0	0	1	0	0	0	0
126	1699	0	0	0	0	0	0	0
138	1836	0	2	0	1	0	0	0
146	1933	0	0	2	0	0	0	1
162	2152	1	0	0	1	0	0	1
170	2279	0	0	0	0	0	0	1
182	2497	0	0	0	0	0	0	0

194	2755	0	0	0	0	0	0	0
206	3054	0	0	1	1	0	0	0
214	3278	1	0	0	0	0	0	0
222	3521	0	4	0	0	0	0	0
230	3780	0	1	0	0	0	0	0
242	4198	0	0	0	0	0	0	0
250	4494	0	0	0	0	0	0	0
258	4804	0	0	0	0	0	0	0
262	4963	0	1	0	0	0	0	0
270	5289	0	2	0	0	0	0	0
278	5626	0	0	0	0	0	0	0
298	6517	0	1	1	0	2	0	2
302	6705	0	1	1	1	0	0	0
310	7090	0	2	0	0	0	0	1
318	7485	0	4	1	0	0	0	0
326	7890	0	0	0	0	0	0	0
330	8094	0	0	0	1	0	0	0
334	8301	0	3	0	0	0	0	0
342	8715	0	2	1	0	0	0	0
346	8921	1	7	1	0	0	0	1
350	9126	1	1	1	0	0	0	0
354	9330	0	1	0	0	0	0	1
362	9727	0	1	0	0	0	0	0
366	9919	0	0	0	0	0	0	0
370	10108	0	1	0	0	0	0	0
374	10292	0	1	1	0	0	0	0
378	10473	0	3	2	1	0	0	0
382	10650	1	7	0	0	0	1	0
386	10823	0	3	1	0	0	0	0
Depth (cm)	**Age (cal yr BP)**	**EF**	**B**	**GA**	**Z**	**ON**	**RA**	**CF**
390	10993	0	6	0	0	0	0	0
394	11160	0	2	0	0	0	0	0
398	11324	0	3	1	0	0	0	1
402	11485	0	1	0	0	0	0	0
410	11800	0	2	0	0	0	0	0
426	12403	0	0	0	0	0	0	0
434	12694	0	2	0	0	0	0	0

442	12980	0	4	0	0	0	0	0
446	13122	0	2	1	0	0	0	0
454	13404	0	4	0	0	0	0	0
462	13683	0	1	0	0	0	0	0
478	14243	0	2	0	0	0	0	0
486	14522	0	9	1	0	0	0	0
490	14662	0	2	2	0	0	0	0
506	15221	0	0	0	1	0	0	0
510	15361	1	2	0	0	0	0	1

Depth (cm)	**Age (cal yr BP)**	**LE**	**TL**	**PT**	**TER**	**IN**	**WO**	**RU**
50	748	0	0	0	0	3	0	0
62	923	0	1	0	0	5	0	0
74	1088	0	0	1	0	4	0	0
90	1290	0	0	0	0	3	0	0
110	1521	0	2	0	0	5	0	0
126	1699	0	1	0	1	10	0	0
138	1836	0	1	0	0	1	0	0
146	1933	0	0	0	0	5	0	0
162	2152	0	2	0	0	3	0	0
170	2279	0	1	0	0	6	0	0
182	2497	0	0	0	0	7	0	0
194	2755	0	6	0	0	7	0	0
206	3054	0	1	0	0	13	0	0
214	3278	0	1	0	0	4	0	0
222	3521	0	0	0	0	4	0	0
230	3780	0	0	0	0	4	0	0
242	4198	0	0	0	0	1	0	0
250	4494	0	1	0	0	1	0	0
258	4804	0	1	0	0	8	0	0
262	4963	0	1	0	0	2	0	0
Depth (cm)	**Age (cal yr BP)**	**LE**	**TL**	**PT**	**TER**	**IN**	**WO**	**RU**
270	5289	0	1	0	0	4	0	0
278	5626	0	1	0	0	11	0	0
298	6517	0	2	0	0	9	0	0
302	6705	0	3	0	0	5	0	0

310	7090	0	1	0	0	7	0	0
318	7485	0	1	0	0	2	0	0
326	7890	0	1	0	0	2	0	0
330	8094	0	1	0	0	1	0	0
334	8301	0	0	0	0	1	0	0
342	8715	0	1	0	0	5	0	0
346	8921	0	0	0	0	3	0	0
350	9126	0	0	0	0	0	0	0
354	9330	0	0	0	0	1	0	0
362	9727	0	0	0	0	3	0	0
366	9919	0	0	0	0	0	0	0
370	10108	0	1	0	0	1	0	0
374	10292	1	0	0	0	4	0	0
378	10473	0	2	0	0	6	2	0
382	10650	0	0	0	0	8	0	0
386	10823	0	0	0	0	13	0	0
390	10993	0	0	1	0	2	0	0
394	11160	0	0	0	0	0	0	0
398	11324	0	0	0	0	5	0	0
402	11485	0	0	0	0	11	0	0
410	11800	0	0	0	0	4	0	0
426	12403	0	0	0	0	4	0	0
434	12694	0	0	1	0	18	0	0
442	12980	0	0	0	0	9	0	0
446	13122	0	0	0	0	7	0	0
454	13404	0	0	0	0	1	0	0
462	13683	0	0	0	0	3	0	0
478	14243	0	0	0	0	19	0	1
486	14522	0	0	0	0	6	0	0
490	14662	0	0	0	0	12	0	0
506	15221	0	0	0	0	8	0	0
510	15361	0	1	0	0	17	0	0

Depth (cm)	**Age (cal yr BP)**	**AP**	**PR**	**SC**	**DY**	**Y**	**MY**	**UP**
50	748	1	0	0	1	0	0	1

62	923	0	0	0	1	0	1	11
74	1088	1	0	0	0	1	0	31
90	1290	1	0	1	0	0	0	13
110	1521	1	0	0	0	0	0	29
126	1699	1	0	1	0	0	0	7
138	1836	0	1	1	0	2	0	8
146	1933	2	0	0	0	0	0	10
162	2152	1	1	1	0	1	0	6
170	2279	2	0	0	1	1	0	5
182	2497	3	0	1	0	0	0	13
194	2755	1	0	0	1	0	1	4
206	3054	1	0	0	0	0	0	11
214	3278	0	0	2	0	3	0	7
222	3521	1	0	0	0	1	0	1
230	3780	0	1	0	0	1	0	4
242	4198	0	0	1	0	1	0	1
250	4494	1	0	1	0	0	1	0
258	4804	0	0	0	0	0	0	1
262	4963	0	0	3	0	2	0	0
270	5289	0	0	2	0	0	0	4
278	5626	2	0	2	1	1	0	4
298	6517	0	0	2	0	0	0	1
302	6705	0	0	5	0	0	0	5
310	7090	0	0	3	2	0	0	0
318	7485	1	0	1	0	0	0	2
326	7890	0	0	3	0	0	0	1
330	8094	0	0	1	0	1	0	4
334	8301	0	0	0	0	0	0	0
342	8715	0	0	0	1	1	0	0
346	8921	1	0	3	0	0	0	0
350	9126	0	0	1	1	0	1	1
354	9330	1	0	1	0	0	0	0
362	9727	0	0	1	0	1	0	4
366	9919	0	0	0	1	0	0	0
370	10108	0	0	1	0	0	1	0
374	10292	1	0	0	3	2	0	0
378	10473	0	0	2	0	2	0	0
382	10650	1	0	0	0	0	0	0

386	10823	1	0	0	0	4	1	1
Depth (cm)	**Age (cal yr BP)**	**PS**	**PD**	**EQ**	**UT**	**SD**	**TY**	**BAR**
390	10993	0	0	0	0	4	1	0
394	11160	1	0	0	0	3	0	0
398	11324	0	1	0	0	2	0	0
402	11485	0	0	0	0	2	0	0
410	11800	0	0	0	0	1	0	0
426	12403	0	1	0	0	15	0	0
434	12694	1	1	0	0	7	0	0
442	12980	0	0	0	1	1	1	0
446	13122	2	0	0	0	6	0	0
454	13404	1	0	0	0	5	0	0
462	13683	1	0	0	2	0	0	0
478	14243	1	0	0	0	5	0	0
Depth	Age	AP	PR	SC	DY	Y	MY	UP
486	14522	1	0	0	2	9	2	0
490	14662	0	1	1	2	6	0	0
506	15221	1	1	0	0	9	0	0
510	15361	1	0	0	2	15	1	1

Depth (cm)	**Age (cal yr BP)**	**PS**	**PD**	**EQ**	**UT**	**SD**	**TY**	**BAR**
50	748	6	16	1	0	0	0	0
62	923	12	8	0	0	0	0	0
74	1088	3	0	3	0	0	0	0
90	1290	3	2	1	0	0	0	0
110	1521	7	22	0	0	0	0	2
126	1699	0	50	0	0	0	0	0
138	1836	9	7	0	0	0	0	0
146	1933	6	90	0	0	0	0	0
162	2152	1	158	0	0	0	0	1
170	2279	4	8	0	0	1	0	0
182	2497	2	517	0	0	0	0	0
194	2755	4	124	0	0	0	0	0
206	3054	0	0	1	0	0	0	1
214	3278	0	4	1	0	0	0	1
222	3521	1	5	1	0	0	0	2

230	3780	0	0	0	0	0	0	0
242	4198	1	2	0	0	0	0	0
250	4494	1	117	0	0	0	0	1
258	4804	0	0	1	0	0	0	0
Depth (cm)	**Age (cal yr BP)**	**PS**	**PD**	**EQ**	**UT**	**SD**	**TY**	**BAR**
262	4963	1	0	0	0	0	0	1
270	5289	2	2	0	0	0	0	0
278	5626	1	14	1	0	0	0	0
298	6517	0	17	0	0	0	0	0
302	6705	3	39	2	0	0	0	1
310	7090	2	13	0	0	0	0	0
318	7485	6	14	0	0	0	0	0
326	7890	1	2	0	0	0	2	1
330	8094	4	5	0	0	0	0	0
334	8301	1	1	0	0	0	0	0
342	8715	2	1	0	0	0	0	0
346	8921	2	4	0	0	0	0	0
350	9126	0	25	0	0	0	0	0
354	9330	0	1	0	0	0	0	0
362	9727	1	8	0	0	0	0	0
366	9919	0	4	0	0	2	0	0
370	10108	2	1	0	0	0	0	0
374	10292	0	2	0	0	1	0	0
378	10473	0	0	0	1	0	0	0
382	10650	0	0	0	0	1	1	0
386	10823	7	4	4	0	0	2	0
390	10993	5	2	1	0	0	0	1
394	11160	0	0	1	0	3	0	0
398	11324	0	0	1	0	0	0	0
402	11485	0	0	3	0	0	0	0
410	11800	2	3	1	0	0	3	0
426	12403	0	0	0	0	0	0	0
434	12694	3	1	1	0	0	0	0
442	12980	0	0	0	0	0	1	0
446	13122	0	0	0	0	0	1	0
454	13404	0	0	1	0	0	1	0
462	13683	0	0	6	0	0	0	0

478	14243	0	0	0	0	1	1	0
486	14522	0	0	0	0	0	0	0
490	14662	0	0	3	0	0	0	0
506	15221	0	0	2	0	0	1	0
510	15361	0	0	1	0	0	1	0

Depth (cm)	**Age (cal yr BP)**	**EU**
50	748	82.5
62	923	71
74	1088	226.5
90	1290	106
110	1521	81
126	1699	91.5
138	1836	55.5
146	1933	55.5
162	2152	74.5
170	2279	52
182	2497	43
194	2755	51
206	3054	68.5
214	3278	55.5
222	3521	45
230	3780	57.5
242	4198	70.5
250	4494	47
258	4804	69.5
262	4963	79
270	5289	72
278	5626	137
298	6517	67
302	6705	98.5
310	7090	51.5
318	7485	84
326	7890	68.5
330	8094	57
334	8301	41.5

342	8715	58
346	8921	44.5
350	9126	38
354	9330	24
362	9727	17.5
366	9919	31.5
370	10108	49
374	10292	37
378	10473	59
382	10650	88.5
386	10823	97
Depth (cm)	**Age (cal yr BP)**	**EU**
390	10993	73
394	11160	77
398	11324	63
402	11485	290.5
410	11800	113
426	12403	124
434	12694	207.5
442	12980	161
446	13122	129
454	13404	163
462	13683	275
478	14243	236.5
486	14522	284.5
490	14662	226
506	15221	263
510	15361	350.5